

# THE [ $^{14}\text{C}$ ]DEOXYGLUCOSE METHOD FOR THE MEASUREMENT OF LOCAL CEREBRAL GLUCOSE UTILIZATION: THEORY, PROCEDURE, AND NORMAL VALUES IN THE CONSCIOUS AND ANESTHETIZED ALBINO RAT<sup>1</sup>

L. SOKOLOFF,<sup>2</sup> M. REIVICH,<sup>4</sup> C. KENNEDY,<sup>2,3</sup> M. H. DES ROSIERS,<sup>2</sup> C. S. PATLAK,<sup>5</sup>  
K. D. PETTIGREW,<sup>5</sup> O. SAKURADA<sup>2</sup> and M. SHINOHARA<sup>2</sup>

<sup>2</sup>Laboratory of Cerebral Metabolism, National Institute of Mental Health, Bethesda, MD 20014, U.S.A.,

<sup>3</sup>Department of Pediatrics, Georgetown University School of Medicine, Washington, DC 20007, U.S.A.,

<sup>4</sup>Department of Neurology, University of Pennsylvania School of Medicine, Philadelphia  
PA 19174, U.S.A.

and

<sup>5</sup>Theoretical Statistics and Mathematics Branch, Division of Biometry and Epidemiology,  
National Institute of Mental Health, Bethesda, MD 20014, U.S.A.

(Received 3 November 1976. Accepted 12 January 1977)

**Abstract**—A method has been developed for the simultaneous measurement of the rates of glucose consumption in the various structural and functional components of the brain *in vivo*. The method can be applied to most laboratory animals in the conscious state. It is based on the use of 2-deoxy-D- [ $^{14}\text{C}$ ]glucose ([ $^{14}\text{C}$ ]DG) as a tracer for the exchange of glucose between plasma and brain and its phosphorylation by hexokinase in the tissues. [ $^{14}\text{C}$ ]DG is used because the label in its product, [ $^{14}\text{C}$ ]deoxyglucose-6-phosphate, is essentially trapped in the tissue over the time course of the measurement. A model has been designed based on the assumptions of a steady state for glucose consumption, a first order equilibration of the free [ $^{14}\text{C}$ ]DG pool in the tissue with the plasma level, and relative rates of phosphorylation of [ $^{14}\text{C}$ ]DG and glucose determined by their relative concentrations in the precursor pools and their respective kinetic constants for the hexokinase reaction. An operational equation based on this model has been derived in terms of determinable variables. A pulse of [ $^{14}\text{C}$ ]DG is administered intravenously and the arterial plasma [ $^{14}\text{C}$ ]DG and glucose concentrations monitored for a preset time between 30 and 45 min. At the prescribed time, the head is removed and frozen in liquid N<sub>2</sub>-chilled Freon XII, and the brain sectioned for autoradiography. Local tissue concentrations of [ $^{14}\text{C}$ ]DG are determined by quantitative autoradiography. Local cerebral glucose consumption is calculated by the equation on the basis of these measured values.

The method has been applied to normal albino rats in the conscious state and under thiopental anesthesia. The results demonstrate that the local rates of glucose consumption in the brain fall into two distinct distributions, one for gray matter and the other for white matter. In the conscious rat the values in the gray matter vary widely from structure to structure (54–197  $\mu\text{mol}/100\text{ g}/\text{min}$ ) with the highest values in structures related to auditory function, e.g. medial geniculate body, superior olive, inferior colliculus, and auditory cortex. The values in white matter are more uniform (i.e. 33–40  $\mu\text{mol}/100\text{ g}/\text{min}$ ) at levels approximately one-fourth to one-half those of gray matter. Heterogeneous rates of glucose consumption are frequently seen within specific structures, often revealing a pattern of cytoarchitecture. Thiopental anesthesia markedly depresses the rates of glucose utilization throughout the brain, particularly in gray matter, and metabolic rate throughout gray matter becomes more uniform at a lower level.

THE MAMMALIAN brain is a complex heterogeneous organ comprising many structural and functional components with different and independently regulated levels of functional activity and energy metabolism. Much of our present knowledge of cerebral

energy metabolism *in vivo* has been obtained by means of the nitrous oxide technique of KETY & SCHMIDT (1948) and its modifications (SCHEINBERG & STEAD, 1949; LASSEN & MUNCK, 1955; EKLÖF *et al.*, 1973; GJEDDE *et al.*, 1975), which measure the average rates of energy metabolism in the brain as a whole. These methods have demonstrated changes in cerebral metabolic rate in association with gross or diffuse alterations of cerebral function and/or structure, as, for example, those that occur during postnatal development, aging, senility, anesthesia, disorders of consciousness, and convulsive states (KETY, 1950, 1957; LASSEN, 1959; SOKOLOFF, 1960, 1976). They have not

<sup>1</sup> Preliminary reports of portions of this work were presented at the 5th Annual Meeting of the American Society for Neurochemistry, New Orleans, March, 1974 (SOKOLOFF *et al.*, 1974; KENNEDY *et al.*, 1974).

Abbreviations used: DG, 2-Deoxy-D-glucose; DG-6-P, 2-deoxy-D-glucose-6-phosphate; G-6-P, glucose-6-phosphate.

detected changes in cerebral metabolic rate in a number of conditions with, perhaps, more subtle alterations in cerebral functional activity, for example, deep slow-wave sleep, performance of mental arithmetic, sedation and tranquilization, schizophrenia, and LSD-induced psychosis (KETY, 1950; LASSEN, 1959; SOKOLOFF, 1969). It is possible that there are no changes in cerebral energy metabolism in these conditions. The apparent lack of change could also be explained by either a redistribution of local levels of functional and metabolic activity without significant change in the average of the brain as a whole or the restriction of altered metabolic activity to regions too small to be detected in measurements of the brain as a whole. The latter possibilities point to the need to measure metabolic rate locally in the individual structural and functional units of the brain.

Some of the methods currently used to measure the rates of cerebral glucose utilization in animals can be applied to local regions of the brain. One is the closed system technique of LOWRY and associates (1964); another is the  $[2-^{14}\text{C}]$ glucose method of HAWKINS *et al.* (1974). These methods are designed, however, primarily for use in the brain as a whole, and the localization possible with them is limited only to structures that can be dissected out cleanly in sufficient amounts to permit the necessary chemical analyses.

Kety and his associates (LANDAU *et al.*, 1955; FREYGANG & SOKOLOFF, 1958; KETY, 1960; REIVICH *et al.*, 1969) developed a quantitative autoradiographic technique to measure the local tissue concentrations of chemically inert, diffusible, radioactive tracers which they used to determine the rates of blood flow simultaneously in all the structural components visible and identifiable in autoradiographs of serial sections of the brain. The application of this quantitative autoradiographic technique to the determination of local cerebral metabolic rate has proved to be more difficult because of the inherently greater complexity of the problem and the unsuitability of the labeled species of the normal substrates of cerebral energy metabolism, oxygen and glucose. The radioisotopes of oxygen have too short a physical half-life; both oxygen and glucose are too rapidly converted to carbon dioxide; and  $\text{CO}_2$  is too rapidly cleared from the cerebral tissues. We have, therefore, utilized 2-deoxy-D- $[^{14}\text{C}]$ glucose, a labeled analogue of glucose with special properties that make it particularly appropriate for this application. It is metabolized through part of the pathway of glucose metabolism at a definable rate relative to that of glucose. Unlike glucose, however, its product,  $[^{14}\text{C}]$ deoxyglucose-6-phosphate, is essentially trapped in the tissues, allowing the application of the quantitative autoradiographic technique.

The present report presents the theory, development, and use of this autoradiographic  $[^{14}\text{C}]$ deoxyglucose technique to determine quantitatively the rates of glucose utilization in the structural and func-

tional components of the brain of conscious and anesthetized laboratory animals.

## THEORY

*Biochemical properties of deoxyglucose.* 2-Deoxy-D-glucose differs from glucose only in the replacement of the hydroxyl group on the second carbon atom by a hydrogen atom. This single structural difference is responsible for the chemical properties that make 2-deoxyglucose so suitable for the present method. The remainder of the molecule is indistinguishable from that of glucose, and it is metabolized qualitatively exactly like glucose until a point in the glycolytic pathway is reached where its anomalous structure prevents its further metabolism. Thus, deoxyglucose is transported between blood and brain tissues by the same saturable carrier that transports glucose (BIDDER, 1968; BACHELARD, 1971; OLDENDORF, 1971; HORTON *et al.*, 1973). In the tissues it competes with glucose for hexokinase which phosphorylates both to their respective hexose-6-phosphates (SOLS & CRANE, 1954). It is at this point in the biochemical pathway that the further metabolism of the two compounds diverges. Glucose-6-phosphate is converted to fructose-6-phosphate by phosphohexoseisomerase and metabolized further via the glycolytic and tricarboxylic acid cycle pathways. 2-Deoxyglucose-6-phosphate cannot be isomerized to fructose-6-phosphate because of the lack of a hydroxyl group on its second carbon atom, and its metabolism, therefore, ceases at this point in the pathway (SOLS & CRANE, 1954; WICK *et al.*, 1957; TOWER, 1958; BACHELARD *et al.*, 1971; HORTON *et al.*, 1973). Although not a substrate for further metabolism, deoxyglucose-6-phosphate does have an affinity for the phosphohexoseisomerase and, when present in sufficiently high concentrations, can competitively inhibit glucose-6-phosphate metabolism at this point (WICK *et al.*, 1957; TOWER, 1958; HORTON *et al.*, 1973). Indeed, it is probably mainly by this competitive inhibition at the phosphohexoseisomerase step that pharmacological doses of deoxyglucose lead to an inhibition of glycolysis and produce a clinical syndrome like that of hypoglycemia (TOWER, 1958; LANDAU & LUBS, 1958; HORTON *et al.*, 1973; MELDRUM & HORTON, 1973); inhibition at the hexokinase step, either competitively by deoxyglucose or by depletion of ATP, may also be contributory (TOWER, 1958; HORTON *et al.*, 1973).

There are alternative pathways of glucose-6-phosphate metabolism, but these do not appear to have significant influence on the fate of deoxyglucose-6-phosphate in brain. Glucose-6-phosphate can be oxidized by glucose-6-phosphate dehydrogenase, the first step in the hexosemonophosphate shunt, but deoxyglucose-6-phosphate does not appear to be a substrate for this enzyme (SOLS & CRANE, 1954; TOWER, 1958; HORTON *et al.*, 1973). Glucose-6-phosphate can also be hydrolyzed back to free glucose by glucose-6-phosphatase. The activity of this enzyme has been reported to be very low in mammalian brain (HERS & DE DUVE, 1950; HERS, 1957; RAGGI *et al.*, 1960; PRASANNAN & SUBRAHMANYAM, 1968), and, as will be discussed below, deoxyglucose-6-phosphatase activity in brain is insufficient to be a factor in the present studies.

*Description of theoretical model.* The theoretical basis of the  $[^{14}\text{C}]$ deoxyglucose technique is derived from the analysis of a model of the biochemical behavior of deoxyglucose in brain. This model is diagrammatically illustrated in Fig. 1. According to the model  $[^{14}\text{C}]$ deoxyglucose and glucose in the plasma share and compete for a common carrier in the blood-brain barrier for transport from

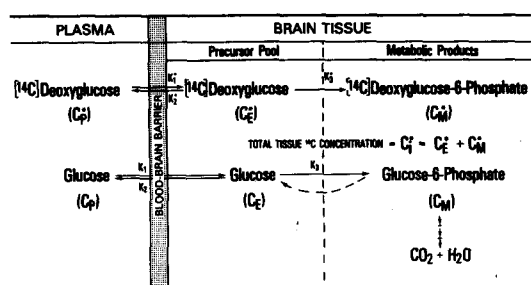


FIG. 1. Diagrammatic representation of the theoretical model.  $C_t^*$  represents the total  $^{14}\text{C}$  concentration in a single homogeneous tissue of the brain.  $C_P^*$  and  $C_P$  represent the concentrations of  $^{14}\text{C}$ deoxyglucose and glucose in the arterial plasma, respectively;  $C_E^*$  and  $C_E$  represent their respective concentrations in the tissue pools that serve as substrates for hexokinase.  $C_M^*$  represents the concentration of  $^{14}\text{C}$ deoxyglucose-6-phosphate in the tissue. The constants  $k_1^*$ ,  $k_2^*$ , and  $k_3^*$  represent the rate constants for carrier-mediated transport of  $^{14}\text{C}$ deoxyglucose from plasma to tissue, for carrier-mediated transport back from tissue to plasma, and for phosphorylation by hexokinase, respectively. The constants  $k_1$ ,  $k_2$ , and  $k_3$  are the equivalent rate constants for glucose.  $^{14}\text{C}$ Deoxyglucose and glucose share and compete for the carrier that transports both between plasma and tissue and for hexokinase which phosphorylates them to their respective hexose-6-phosphates. The dashed arrow represents the possibility of glucose-6-phosphate hydrolysis by glucose-6-phosphatase activity, if any. For more detailed description and analysis of the model, see Theory section.

plasma to brain.  $^{14}\text{C}$ Deoxyglucose and glucose, transported into a homogeneous tissue, enter a common precursor pool in which they compete either for the carrier for transport back from brain to plasma or for the enzyme, hexokinase, which phosphorylates them to  $^{14}\text{C}$ DG-6-P and G-6-P, respectively. The hexokinase reaction is essentially irreversible, and inasmuch as  $^{14}\text{C}$ DG-6-P is not a suitable substrate for any other enzymes known to be present, it is trapped and accumulates as it is formed. On the other hand, G-6-P does not accumulate but is metabolized further eventually to carbon dioxide and water. The model allows for the possibility that a fraction of the G-6-P is hydrolyzed back to free glucose by glucose-6-phosphatase activity (broken arrow in Fig. 1).

The essential qualitative features of the model are firmly founded on the experimentally established biochemical behavior of deoxyglucose in cerebral metabolism described above. The application of the model to the quantification of local cerebral glucose utilization is dependent, however, on the validity of some additional assumptions and/or conditions:

(1) The model is applicable only to a localized region of tissue that is homogeneous with respect to the following: rate of blood flow; rates of transport of  $^{14}\text{C}$ DG and glucose between plasma and tissue; concentrations of  $^{14}\text{C}$ DG, glucose,  $^{14}\text{C}$ DG-6-P, and G-6-P; and rate of glucose utilization.

(2) The  $^{14}\text{C}$ DG and  $^{14}\text{C}$ DG-6-P are present in tracer amounts (i.e. their molecular concentrations in blood and/or tissues are quantitatively negligible and pharmacologically inactive).

(3) To facilitate mathematical analysis of the model it is assumed that all of the free  $^{14}\text{C}$ DG and glucose in each homogeneous element of tissue is present in a single compartment in which their concentrations are those of the precursor pools for the hexokinase reaction and the carrier-mediated transport from tissue to plasma. Inasmuch as there are extracellular and intracellular spaces and multiple cell types in each such element of tissue, this assumption is not fully valid. It will be seen below, after the operational equation is derived and the finally adopted procedure is described, that the design of the procedure serves to minimize, if not eliminate, possible errors arising from invalidity of this assumption.

(4) Carbohydrate metabolism in the brain is in a steady state. The plasma glucose concentration, the rate of local cerebral glucose utilization, and the concentrations of the intermediates of the glycolytic pathway remain constant throughout the period of measurement.

(5) The capillary plasma concentrations of  $^{14}\text{C}$ -deoxyglucose and glucose are approximately equal to or bear a constant relationship to their arterial plasma concentrations. Experiments in this laboratory have demonstrated that the cerebral extraction ratio of  $^{14}\text{C}$ deoxyglucose is normally very low, approx 5%; the mean capillary plasma concentration cannot differ, therefore, by more than 5% from the arterial plasma level. In the case of glucose a constant relationship between arterial and capillary concentrations is implicit in the assumption of steady state conditions for glucose delivery and metabolism.

An essential premise of the model is that the  $^{14}\text{C}$ -DG-6-P is effectively trapped in the tissue for the duration of the period of measurement. Evidence from the literature to support this premise is largely indirect and inferential. It is based mainly on reports that DG-6-P is a poor substrate for enzymes known to exist in brain in significant amounts and that the activities of enzymes for which it might be expected to be a good substrate appear to be negligible in brain. Because of the critical importance of this premise, experiments were carried out to test it directly.

The activity of glucose-6-phosphatase, an enzyme that might be expected to hydrolyze  $^{14}\text{C}$ DG-6-P, is generally believed to be very low in mammalian brain. For example, HERS (1957) found a maximal rate of glucose-6-phosphate hydrolysis of only  $0.06 \mu\text{mol/g/min}$  in rat brain homogenates assayed at  $37^\circ\text{C}$ , at an optimal pH of 6.5, and with saturating concentrations of substrate. Even this maximal rate, which might be expected to be considerably greater than the rate under more physiological conditions of pH and substrate concentration *in vivo*, is only approx 5% of the glycolytic flux *in vivo* in the brain of the conscious rat (see below). To test the possibility that DG-6-P hydrolysis might be more rapid, we carried out similar experiments, at a pH of 7.4 and with saturating concentrations of  $^{14}\text{C}$ DG-6-P as the substrate. The maximal rate of hydrolysis was even lower,  $0.03 \mu\text{mol/g/min}$ , indicating that deoxyglucose-6-phosphatase activity did not present a serious problem.

The possibility was considered that  $^{14}\text{C}$ DG-6-P might be cleared directly from the tissues by the circulation without prior hydrolysis. This possibility was examined in cats. Under light halothane anesthesia a femoral artery and vein were catheterized, and the confluence of the cerebral

venous sinuses was cannulated for the sampling of cerebral venous blood. Two to 4 h after recovery from the anesthesia a pulse of [ $^{14}\text{C}$ ]DG was administered via the femoral venous catheter, and timed samples of arterial and cerebral venous blood were drawn. The blood samples were centrifuged, and their plasma fractions were assayed for  $^{14}\text{C}$  concentrations in a liquid scintillation counter. Despite the rapidly falling arterial and cerebral venous concentrations, there was initially a positive cerebral arteriovenous difference, indicating net uptake of  $^{14}\text{C}$  by the brain. This difference diminished gradually until at approx 7 min the arterial and cerebral venous curves intersected, and a negative arteriovenous difference appeared that persisted for at least 25 min. The plasma samples taken during the period of the negative cerebral arteriovenous difference were analyzed by ion-exchange column chromatography, paper chromatography, and TLC for their [ $^{14}\text{C}$ ]DG and [ $^{14}\text{C}$ ]DG-6-P contents. There was no trace of [ $^{14}\text{C}$ ]DG-6-P in any of the samples. Despite the fact that there was clearly a net loss of  $^{14}\text{C}$  from the brain to the blood during this period, all of the loss could be accounted for as [ $^{14}\text{C}$ ]DG. These results not only confirmed that there is bi-directional transport of free [ $^{14}\text{C}$ ]DG between blood and brain but demonstrated that there is no direct loss of [ $^{14}\text{C}$ ]DG-6-P from the cerebral tissues to the blood.

Although the results of assays of brain homogenates *in vitro* indicated very little deoxyglucose-6-phosphatase activity, there remained a possibility that *in vivo* there might be in some cerebral tissues significant hydrolysis of [ $^{14}\text{C}$ ]DG-6-P and subsequent clearance of the released [ $^{14}\text{C}$ ]DG from the tissue by the circulation. Experiments were, therefore, carried out to estimate the rates of disappearance of [ $^{14}\text{C}$ ]DG-6-P from the various structural components of the brain. A group of rats, matched for age and weight, were anesthetized with halothane, and a femoral artery and vein of each animal were catheterized. Four hours after recovery from anesthesia, the animals were administered equal intravenous pulses of [ $^{14}\text{C}$ ]DG. The arterial plasma [ $^{14}\text{C}$ ]DG concentration of each animal was monitored by liquid scintillation counting and found to reach very low levels by 6 h after the pulse. Animals were killed by decapitation at 6, 17, and 24 h after the pulse, their brains were removed and frozen in Freon XII chilled to  $-75^\circ\text{C}$  in liquid nitrogen, and the local cerebral tissue concentrations of  $^{14}\text{C}$  were determined by the quantitative autoradiographic procedure described below. By 17 h the plasma concentrations had reached and remained at negligible levels long enough for any free [ $^{14}\text{C}$ ]DG in the cerebral tissues to have been cleared by the circulation or metabolized to [ $^{14}\text{C}$ ]DG-6-P. Any loss of  $^{14}\text{C}$  from the tissues thereafter could reasonably be assumed to represent the loss of [ $^{14}\text{C}$ ]DG-6-P and/or its labeled products. The  $^{14}\text{C}$  concentrations in a variety of gray and white cerebral structures at 17 and 24 h after the pulse were, therefore, plotted semi-logarithmically and their half-lives estimated. The mean half-lives in gray and white matter were 7.7 (S.D. =  $\pm 1.6$ ) and 9.7 (S.D. =  $\pm 2.6$ ) h, respectively. The shortest half-life, which was found in the inferior colliculus, was 6.1 h. These results indicate that the loss of  $^{14}\text{C}$  from [ $^{14}\text{C}$ ]DG-6-P in cerebral tissues is sufficiently slow that it could be considered to be essentially trapped if the experimental procedure were limited to less than 1 h. As will be discussed below, the validity of this assumption was further supported by the findings of equal values for local cerebral glucose utilization obtained during experimental intervals of 30 and 45 min.

**Mathematical analysis of model.** At any time following the introduction of [ $^{14}\text{C}$ ]DG into the blood,  $C_t^*$ , the total content of  $^{14}\text{C}$  per unit mass of any tissue,  $i$ , is equal to the sum of the concentrations of the free [ $^{14}\text{C}$ ]DG in the precursor pool in the tissue,  $C_E^*$ , and its product, [ $^{14}\text{C}$ ]deoxyglucose-6-phosphate,  $C_M^*$ , in that tissue (Fig. 1).

Therefore,

$$C_t^* = C_E^* + C_M^* \quad (1)$$

and the derivative of Equation (1) with respect to time,  $t$ , is

$$dC_t^*/dt = dC_E^*/dt + dC_M^*/dt. \quad (2)$$

The rate of change of the free [ $^{14}\text{C}$ ]DG concentration in the tissue,  $dC_E^*/dt$ , is equal to the difference between the rates of its transport into the tissue from the plasma and its loss from the tissue by transport back to the plasma or by hexokinase-catalyzed phosphorylation to [ $^{14}\text{C}$ ]DG-6-P. This relationship can be described by the equation,

$$dC_E^*/dt = k_1^* C_p^* - k_2^* C_E^* - k_3^* C_E^* \quad (3)$$

where  $C_p^*$  equals the concentration of [ $^{14}\text{C}$ ]deoxyglucose in the arterial plasma, and  $k_1^*$ ,  $k_2^*$ , and  $k_3^*$  are the rate constants for the transport of [ $^{14}\text{C}$ ]DG from plasma to brain tissue, for the transport of free [ $^{14}\text{C}$ ]DG back from tissue to plasma, and for the phosphorylation of [ $^{14}\text{C}$ ]DG in the tissue, respectively. The term in which each rate constant appears represents, of course, the rate of the process to which it applies.

It should be noted that  $C_p^*$  actually represents mean capillary rather than arterial plasma concentration. Capillary concentration, however, is not readily measured. Inasmuch as the difference between arterial and cerebral venous [ $^{14}\text{C}$ ]DG concentrations is generally less than 5% of the arterial level, the mean capillary plasma concentration can reasonably closely be approximated by the arterial plasma concentration. Furthermore, as will be seen below, any potential error associated with this approximation is partially counteracted by a corresponding approximation made for the plasma glucose concentration.

The assumption of first order rate constants,  $k_1^*$ ,  $k_2^*$ , and  $k_3^*$ , in the mathematical description of saturable processes, such as carrier-mediated transport and enzyme-catalyzed reactions, might appear to be questionable. With saturable processes first order kinetics apply to only a narrow range of the lowest substrate concentrations. The basic requirements and assumptions of the model presented above provide conditions, however, in which  $k_1^*$ ,  $k_2^*$ , and  $k_3^*$  behave as true first order rate constants. For example, [ $^{14}\text{C}$ ]deoxyglucose and glucose compete for the same carrier for transport from plasma into brain. The rate of inward transport of [ $^{14}\text{C}$ ]DG can, therefore, be described by the classical Michaelis-Menten equation, modified for the influence of the presence of the competitive substrate, glucose (DIXON & WEBB, 1964). Thus,

$$v_i^* = \frac{V_M^* C_p^*}{K_M^* (1 + C_p/K_M) + C_p^*} \quad (4)$$

where  $v_i^*$  = the rate of inward transport of [ $^{14}\text{C}$ ]deoxyglucose,  $V_M^*$  = the maximal velocity of [ $^{14}\text{C}$ ]deoxyglucose transport,  $K_M^*$  and  $K_M$  are the apparent Michaelis-Menten constants of the carrier for [ $^{14}\text{C}$ ]deoxyglucose and glucose, respectively, and  $C_p^*$  and  $C_p$  are the plasma concentrations of [ $^{14}\text{C}$ ]deoxyglucose and glucose, respectively.

The model, however, requires that the [ $^{14}\text{C}$ ]deoxyglu-

cose be administered in tracer amounts and that tracer theory apply.  $C_p^*$  can, therefore, be considered to be negligible compared to  $K_M^* (1 + C_p/K_M)$  and thus

$$v_i^* = \left[ \frac{V_M^*}{K_M^* (1 + C_p/K_M)} \right] C_p^* \quad (5)$$

In Equation (3) it is assumed that

$$v_i^* = k_1^* C_p^* \quad (6)$$

Equating Equations (5) and (6)

$$k_1^* = \left[ \frac{V_M^*}{K_M^* (1 + C_p/K_M)} \right] \quad (7)$$

The model also requires a steady state of cerebral glucose utilization and a constant arterial plasma glucose concentration, i.e. a constant  $C_p$ . It is apparent then that within the constraints imposed by the model  $k_1^*$  is a constant independent of the plasma [ $^{14}\text{C}$ ]DG concentration and, therefore, a true first order rate constant.

By comparable analyses  $k_2^*$  and  $k_3^*$  can be similarly defined and shown to be true rate constants as used in Equation (3). Equation (3) can, therefore, be integrated and solved for  $C_E^*$  as a function of time as follows:

$$C_E^*(T) = k_1^* e^{-(k_2^* + k_3^*)T} \int_0^T C_p^* e^{(k_2^* + k_3^*)t} dt \quad (8)$$

where  $T$  = any given time following the introduction of the [ $^{14}\text{C}$ ]deoxyglucose into the circulation.

The tissue concentration of [ $^{14}\text{C}$ ]DG-6-P as a function of time can also be mathematically described.  $dC_M^*/dt$  equals the rate of formation and accumulation of [ $^{14}\text{C}$ ]DG-6-P per unit mass of tissue. Thus

$$dC_M^*/dt = k_3^* C_E^* \quad (9)$$

Substituting for  $C_E^*$  its equivalent function defined in Equation (8) and integrating and solving for  $C_M^*$ ,

$$C_M^*(\tau) = k_1^* k_3^* \int_0^\tau \left[ e^{-(k_2^* + k_3^*)T} \int_0^T C_p^* e^{(k_2^* + k_3^*)t} dt \right] dT \quad (10)$$

where  $\tau$  = any given time following the introduction of the [ $^{14}\text{C}$ ]deoxyglucose into the circulation.

The functions for  $C_E^*$  and  $C_M^*$  defined in Equations (8) and (10), respectively, can now be substituted for these variables in Equation (1) to obtain the following equation,

$$C_i^*(\tau) = k_1^* e^{-(k_2^* + k_3^*)\tau} \int_0^\tau C_p^* e^{(k_2^* + k_3^*)t} dt + k_1^* k_3^* \int_0^\tau \left[ e^{-(k_2^* + k_3^*)T} \int_0^T C_p^* e^{(k_2^* + k_3^*)t} dt \right] dT \quad (11)$$

Equation (11) defines the total tissue concentration of  $^{14}\text{C}$  as a function of time in terms of the history of the plasma concentration from zero time to any given time,  $\tau$ , and the rate constants,  $k_1^*$ ,  $k_2^*$ , and  $k_3^*$ . The application of this equation to the determination of the rate constants will be described below.

The behavior of glucose is similar to that of [ $^{14}\text{C}$ ]deoxyglucose, but its mathematical description is simpler because of the assumptions of a constant arterial plasma glucose concentration and a steady state of glucose uptake and metabolism in brain. Thus,

$$dC_E/dt = k_1 C_p - k_2 C_E - k_3 C_E \quad (12)$$

where  $C_p$  and  $C_E$  represent the free glucose concentrations

in arterial plasma and brain tissue, respectively, and  $k_1$ ,  $k_2$  and  $k_3$  represent the rate constants for transport of glucose from plasma to tissue, for transport back from tissue to plasma, and for the phosphorylation of free glucose in the tissue to G-6-P by hexokinase, respectively.

Again, as in the case of [ $^{14}\text{C}$ ]DG,  $C_p$  should represent mean capillary plasma glucose concentration but can be approximated by the arterial plasma concentration because of the generally low net extraction of glucose from cerebral blood. Furthermore, as can be seen in the operational equation developed below, on which the method is based, it is the ratio of plasma [ $^{14}\text{C}$ ]deoxyglucose and glucose concentrations that is most critical. The application of the same approximation to both substances tends, therefore, to cancel the effects of the approximations.

The constants,  $k_1$ ,  $k_2$  and  $k_3$ , also behave as first order rate constants. With saturable processes such as carrier-mediated transport and enzyme-catalysed reactions, they are obviously influenced by the plasma and tissue concentrations of glucose. The model requires, however, steady state conditions, for example, constant plasma and tissue concentrations of glucose, throughout the duration of the procedure. Under those circumstances,  $k_1$ ,  $k_2$  and  $k_3$  become constants of proportionality between the constant rates of the process and the constant glucose concentrations in the pools to which they apply.

The assumption of a steady state also means that  $dC_E/dt$  in Equation (12) equals zero. Equation (12) can then be solved as follows:

$$C_E = [k_1/(k_2 + k_3)] C_p \quad (13)$$

The combination of constants,  $k_1/(k_2 + k_3)$  is, therefore, equal to the distribution ratio of glucose between the tissue and plasma in the steady state. It is equivalent to the tissue-plasma-partition coefficient or, more appropriately, the distribution volume for glucose per unit mass of tissue.

*Derivation of operational equation.* The analysis of the model has been further extended to derive an operational equation that defines the variables to be measured and the procedures to be followed to determine local cerebral glucose utilization. The derivation begins with the Fick principle, which states that the rate of uptake or loss of a substance from a tissue is equal to the difference between its rates of delivery to the tissue in the arterial blood and its removal in the venous blood. Applied to the  $^{14}\text{C}$  introduced into the blood as [ $^{14}\text{C}$ ]deoxyglucose, this principle can be stated as follows:

$$F(C_A^* - C_V^*) = dC_i^*/dt \quad (14)$$

where  $F$  = the rate of blood flow per unit mass of the  $i$ th tissue, and  $C_A^*$  and  $C_V^*$  are the concentrations of  $^{14}\text{C}$  in the arterial blood and the venous blood draining that tissue, respectively.

Combining Equation (14) with Equation (2) and substituting  $v^*$  for  $dC_M^*/dt$ , which is the rate of phosphorylation of [ $^{14}\text{C}$ ]DG by hexokinase,

$$F(C_A^* - C_V^*) = dC_i^*/dt = dC_E^*/dt + v^* \quad (15)$$

Because of the steady state conditions, the net uptake of glucose from the blood is equal to the rate of glucose utilization in the tissue. Thus, according to the Fick principle,

$$F(C_A - C_V) = R_i \quad (16)$$

where  $C_A$  and  $C_V$  are the glucose concentrations in the

arterial and venous blood, respectively, and  $R_i$  is the net rate of glucose utilization in the tissue.

In a steady state the net rate of G-6-P formation is equal to the rate of glucose utilization. The net rate of G-6-P formation equals the difference between the rate of glucose phosphorylation by hexokinase and G-6-P dephosphorylation by phosphatase activity, if any.

Therefore,

$$R_i = v - r \quad (17)$$

where  $v$  = the rate of phosphorylation of glucose, and  $r$  = the rate of G-6-P hydrolysis, indicated by the dashed arrow in Fig. 1.

Factoring out  $v$  in Equation (17)

$$R_i = (1 - r/v)v = \phi v \quad (18)$$

where  $\phi = 1 - r/v$ .

In a steady state  $v$  and  $r$  are constants. Therefore,  $\phi$  is also a constant between zero and one that represents the fraction of glucose that once phosphorylated is metabolized further, and  $\phi v$  equals the rate of glucose utilization. Inasmuch as there is little glucose-6-phosphatase in brain,  $\phi$  can be expected to be very close to one.

Dividing Equation [15] by  $F(C_A - C_V)$  or its equivalents defined in Equations [16] and [18],

$$\frac{F(C_A^* - C_V^*)}{F(C_A - C_V)} = \frac{dC_i^*/dt}{R_i} = \frac{dC_E^*/dt}{R_i} + \frac{v^*}{\phi v} \quad (19)$$

It can be seen from the left side of Equation (19) that it represents the ratio of the net uptakes of [ $^{14}\text{C}$ ]DG and glucose by the tissue from the blood.

[ $^{14}\text{C}$ ]Deoxyglucose and glucose are competitive substrates for hexokinase, and  $v^*$  and  $v$  represent their rates of phosphorylation, respectively, under these conditions of mutual competitive inhibition. Solution of the rate equations for two substrates competing for the same enzyme leads to the classical Michaelis-Menten relationship, modified to take into account the influence of the competitive substrate (DIXON & WEBB, 1964). Thus,

$$v^*/v = \frac{\frac{C_E^* V_m^*}{K_m^*(1 + C_E/K_m) + C_E^*}}{\frac{C_E V_m}{K_m(1 + C_E/K_m) + C_E}} \quad (20)$$

where  $V_m^*$  and  $V_m$  are the maximal velocities,  $K_m^*$  and  $K_m$  are the apparent Michaelis-Menten constants, and  $C_E^*$  and  $C_E$  are the substrate concentrations for [ $^{14}\text{C}$ ]deoxyglucose and glucose, respectively, in the hexokinase reactions.

With tracer amounts of [ $^{14}\text{C}$ ]deoxyglucose, however,  $C_E^*$  is negligible. Therefore,

$$K_m^*(1 + C_E/K_m) + C_E^* \approx K_m^*(1 + C_E/K_m) \quad (21)$$

and

$$K_m(1 + C_E^*/K_m) + C_E \approx K_m + C_E = K_m(1 + C_E/K_m). \quad (22)$$

Therefore, Equation (20) reduces to

$$v^*/v = \frac{\frac{C_E^* V_m^*}{K_m^*(1 + C_E/K_m)}}{\frac{C_E V_m}{K_m(1 + C_E/K_m)}} \quad (23)$$

and after cancellation and rearrangement

$$v^*/v = (C_E^*/C_E) \left( \frac{V_m^* K_m}{V_m K_m^*} \right). \quad (24)$$

Substituting for  $v^*/v$  in Equation (19) and rearranging

$$\frac{dC_i^*/dt - dC_E^*/dt}{R_i} = (C_E^*/C_E) \left( \frac{V_m^* K_m}{\phi V_m K_m^*} \right). \quad (25)$$

$C_E^*$  and  $C_E$  are defined in Equations (8) and (13). Dividing Equation (8) by Equation (13),

$$C_E^*/C_E = \frac{k_1^* e^{-(k_2^* + k_3^*)T} \int_0^T C_P^* e^{(k_2^* + k_3^*)t} dt}{[k_1/(k_2 + k_3)] C_P} \quad (26)$$

Multiplying the numerator by  $(k_2^* + k_3^*)/(k_2^* + k_3^*)$  and dividing through by  $C_P$ , which is a constant and can, therefore, be incorporated under the integral,

$$C_E^*/C_E = \lambda(k_2^* + k_3^*) e^{-(k_2^* + k_3^*)T} \int_0^T (C_P^*/C_P) e^{(k_2^* + k_3^*)t} dt \quad (27)$$

where  $\lambda$  represents the constant,

$$\frac{k_1^*/(k_2^* + k_3^*)}{k_1/(k_2 + k_3)},$$

which is equal to the ratio of the distribution volumes for [ $^{14}\text{C}$ ]deoxyglucose and glucose in the tissue.

Substituting for  $C_E^*/C_E$  in Equation (25), rearranging, and integrating from zero time to the final time,  $\tau$ ,

$$C_i^*(\tau) - C_E^*(\tau) = R_i \int_0^\tau \left[ \lambda(k_2^* + k_3^*) e^{-(k_2^* + k_3^*)T} \times \int_0^T (C_P^*/C_P) e^{(k_2^* + k_3^*)t} dt \right] dT \left( \frac{V_m^* K_m}{\phi V_m K_m^*} \right). \quad (28)$$

Substituting for  $C_E^*$  its equivalent function defined in Equation (8), and solving for  $R_i$ ,

$$R_i = \frac{C_i^*(\tau) - k_1^* e^{-(k_2^* + k_3^*)\tau} \int_0^\tau C_P^* e^{(k_2^* + k_3^*)t} dt}{\left( \frac{\lambda V_m^* K_m}{\phi V_m K_m^*} \right) \int_0^\tau \left[ (k_2^* + k_3^*) e^{-(k_2^* + k_3^*)T} \times \int_0^T (C_P^*/C_P) e^{(k_2^* + k_3^*)t} dt \right] dT}. \quad (29)$$

The denominator of Equation (29) can be integrated by parts to yield the following simpler and more useful form of the equation:

$$R_i = \frac{C_i^*(\tau) - k_1^* e^{-(k_2^* + k_3^*)\tau} \int_0^\tau C_P^* e^{(k_2^* + k_3^*)t} dt}{\left( \frac{\lambda V_m^* K_m}{\phi V_m K_m^*} \right) \left[ \int_0^\tau (C_P^*/C_P) dt - e^{-(k_2^* + k_3^*)\tau} \times \int_0^\tau (C_P^*/C_P) e^{(k_2^* + k_3^*)t} dt \right]}. \quad (30)$$

Equation (30) is the operational equation of the method. It states that if [ $^{14}\text{C}$ ]DG is introduced into the blood and allowed to circulate for time,  $\tau$ , then the rate of glucose consumption,  $R_i$ , in any cerebral tissue,  $i$ , can be calculated, provided that the total concentration of [ $^{14}\text{C}$ ] in that tissue,  $C_i^*$ , is measured at time  $\tau$ , the entire histories of the arterial plasma concentrations of [ $^{14}\text{C}$ ]DG and glucose from zero time to time,  $\tau$ , are determined, and the rate constants,  $k_1^*$ ,  $k_2^*$ , and  $k_3^*$ , and the single lumped constant, a combination of six other constants, are known. The necessary conditions for Equation (30) to apply are that the [ $^{14}\text{C}$ ]DG be present in tracer amounts, that the arterial plasma glucose concentration remain constant, and that the glucose

metabolism of the tissue be in a steady state during the period of measurement.

*Theoretical basis for determination of rate constants.* Equation (11) provides the theoretical basis for the determination of the rate constants,  $k_1^*$ ,  $k_2^*$ , and  $k_3^*$ . It describes the time course of the total concentration of  $^{14}\text{C}$  in a tissue as a function of time, the time course of the plasma [ $^{14}\text{C}$ ]DG concentration, and the three rate constants. Time courses of tissue  $^{14}\text{C}$  and plasma [ $^{14}\text{C}$ ]DG concentrations can be experimentally determined, and then nonlinear, least-squares routines can be used to fit Equation (11) to the experimental data and compute the best-fitting values of  $k_1^*$ ,  $k_2^*$ , and  $k_3^*$ . This approach was used in the present studies; the details are presented below in the Methods section.

*Theoretical basis for determination of lumped constant.* The lumped constant combines six constants into one. To determine even that one constant separately in each of the structural components of the brain would represent, however, a formidable undertaking. Fortunately, the composition of the lumped constant is such that it can reasonably be assumed to be relatively uniform throughout the brain. For example, the lumped constant,  $[\lambda V_m^* K_m / \phi V_m K_m^*]$ , is really the product of four factors,  $1/\phi$ ,  $\lambda$ ,  $V_m^*/V_m$ , and  $K_m/K_m^*$ . The first factor is the reciprocal of  $\phi$ , a constant between zero and one that reflects the amount of glucose-6-phosphatase activity; in view of the almost negligible activity of this enzyme in brain (HERS, 1957),  $\phi$  is likely to be equal or close to one throughout the brain. The second factor,  $\lambda$ , represents the ratio of distribution volumes for [ $^{14}\text{C}$ ]DG and glucose in the tissue. Although the distribution volume for [ $^{14}\text{C}$ ]DG varies in the different tissues of the brain (Table 1), the distribution volume for glucose probably varies proportionately so that the ratio,  $\lambda$ , can be expected to remain constant throughout the brain.  $V_m^*/V_m$  is the ratio of the maximal velocities of phosphorylation of [ $^{14}\text{C}$ ]DG and glucose by hexokinase. Maximal velocity reflects total amount of enzyme, which almost certainly varies from tissue to tissue, but then the two maximal velocities would vary in proportion so that  $V_m^*/V_m$  remains constant. Similarly, the ratio of the Michaelis-Menten constants,  $K_m/K_m^*$ , which represent kinetic properties of the enzyme, can be expected to be uniform throughout the brain. It is likely, therefore, that a lumped constant determined for the brain as a whole would be representative of the lumped constants in its component parts.

Appropriate manipulation of the equations developed above leads to a mathematical definition of the lumped constant for the whole brain in terms of measurable physiological variables.

After cancellation of  $F$ , Equation (19) can be rewritten as follows:

$$\frac{(C_A^* - C_V^*)}{(C_A - C_V)} = \frac{dC_E^*/dT}{R_i} + \frac{v^*}{\phi v} \quad (31)$$

Factoring out  $C_A^*$  and  $C_A$  leads to

$$\left(\frac{C_A^*}{C_A}\right)\left(\frac{E^*}{E}\right) = \frac{dC_E^*/dT}{R_i} + \frac{v^*}{\phi v} \quad (32)$$

where  $E^*$  and  $E$  equal  $(C_A^* - C_V^*)/C_A^*$  and  $(C_A - C_V)/C_A$ , the cerebral extraction ratios for [ $^{14}\text{C}$ ]DG and glucose, respectively.

Substituting for  $v^*/v$  its equivalent function defined in

Equation (24),

$$\left(\frac{C_A^*}{C_A}\right)\left(\frac{E^*}{E}\right) = \frac{dC_E^*/dT}{R_i} + \frac{C_E^*}{C_E} \left(\frac{V_m^* K_m}{\phi V_m K_m^*}\right) \quad (33)$$

And substituting for  $C_E^*/C_E$  according to Equation (27),

$$\left(\frac{C_A^*}{C_A}\right)\left(\frac{E^*}{E}\right) = \frac{dC_E^*/dT}{R_i} + (k_2^* + k_3^*) e^{-(k_2^* + k_3^*)T} \times \int_0^T (C_P^*/C_P) e^{(k_2^* + k_3^*)t} dt \left(\frac{\lambda V_m^* K_m}{\phi V_m K_m^*}\right) \quad (34)$$

$C_P$ , the arterial plasma glucose concentration, is already assumed to be constant, and if  $C_P^*$  can also be maintained constant from zero time to any time,  $T$ , then the integration in Equation (34) can be performed explicitly to yield

$$\left(\frac{C_A^*}{C_A}\right)\left(\frac{E^*}{E}\right) = \frac{dC_E^*/dT}{R_i} + \left(\frac{C_P^*}{C_P}\right) [1 - e^{-(k_2^* + k_3^*)T}] \left(\frac{\lambda V_m^* K_m}{\phi V_m K_m^*}\right) \quad (35)$$

If  $C_P^*$  is a constant, then integration of Equation (3) yields

$$C_E^* = \left(\frac{k_1^*}{k_2^* + k_3^*}\right) C_P^* [1 - e^{-(k_2^* + k_3^*)T}] \quad (36)$$

which when differentiated leads to

$$dC_E^*/dT = k_1^* C_P^* e^{-(k_2^* + k_3^*)T} \quad (37)$$

Substituting for  $dC_E^*/dT$  in Equation (35),

$$\left(\frac{C_A^*}{C_A}\right)\left(\frac{E^*}{E}\right) = \frac{k_1^* C_P^* e^{-(k_2^* + k_3^*)T}}{R_i} + \left(\frac{C_P^*}{C_P}\right) \times [1 - e^{-(k_2^* + k_3^*)T}] \left(\frac{\lambda V_m^* K_m}{\phi V_m K_m^*}\right) \quad (38)$$

As  $T$  approaches infinity, then all the terms containing the exponential factor approach zero, and at  $T = \infty$ ,

$$\left(\frac{C_A^*}{C_A}\right)\left(\frac{E^*}{E}\right)(\infty) = \left(\frac{C_P^*}{C_P}\right) \left(\frac{\lambda V_m^* K_m}{\phi V_m K_m^*}\right) \quad (39)$$

And

$$\left(\frac{\lambda V_m^* K_m}{\phi V_m K_m^*}\right) = \left(\frac{E^*}{E}\right) \left(\frac{C_A^*}{C_A}\right) \left(\frac{C_P}{C_P^*}\right)(\infty) \quad (40)$$

Equations (38) and (40) prescribe the procedure to determine the lumped constant. They state that if [ $^{14}\text{C}$ ]DG is so administered to the animal that  $C_P^*$  is maintained constant long enough for the exponential factor,  $e^{-(k_2^* + k_3^*)T}$ , to approach zero, then the ratio of the fractional extractions of [ $^{14}\text{C}$ ]DG and glucose by the brain multiplied by the ratio of the specific activities (i.e. ratio of [ $^{14}\text{C}$ ]DG to glucose concentrations) in arterial blood and plasma declines exponentially with a rate constant equal to  $(k_2^* + k_3^*)$  until it reaches an asymptotic value equal to the lumped constant. The factor,  $(C_A^*/C_A)/(C_P/C_P^*)$ , merely takes into account the possibility that [ $^{14}\text{C}$ ]DG and glucose may distribute disproportionately between plasma and red cells; in the rat this ratio has been found to equal approximately one by the time the asymptotic level is reached.

As described in the Methods section, the lumped constant has been measured by a procedure designed on the basis of this theoretical analysis.

## METHODS

**Chemicals.** 2-Deoxy-D-[1- $^{14}$ C]glucose (spec. act., 50–56 mCi/mmol), 3-O-[1- $^{14}$ C]methyl-D-glucose (spec. act., 53 mCi/mmol), and [N-methyl- $^{14}$ C]antipyrine (11–20 mCi/mmol) were obtained from New England Nuclear Corp., Boston, MA. All radiochemicals were analyzed by paper and/or thin layer chromatography before use and found to be at least 99% radiochemically pure. Enzymes and reagents used in the assay of blood and plasma glucose concentrations were purchased in kit form from Calbiochem, Richmond, CA or Worthington Biochemical Corp., Freehold, NJ. Calibrated [ $^{14}$ C]toluene, used for internal standardization of radioactive samples counted in the liquid scintillation counter, were obtained from Packard Instrument Co., Downers Grove, IL and New England Nuclear Corp., Boston, MA.

**Animals.** All studies in the present report were carried out on normal, adult, male Sprague–Dawley rats weighing between 325 and 450 g. The animals were maintained on Purina Laboratory Chow and water *ad lib.* prior to the study. Experiments in which plasma glucose concentration varied systematically more than 10% during the procedure were excluded because of violation of the theoretical requirement of a constant plasma concentration. In some cases the animals were deprived of food for approx 16 h prior to the study; the fasting tended to stabilize the plasma glucose concentration but had no apparent effect on local cerebral glucose utilization.

Surgical preparation of the animals for the experiments was carried out under light halothane anesthesia. Polyethylene catheters were inserted in one femoral artery and one femoral vein in all animals. The procedure to determine the lumped constant also required the sampling of representative cerebral venous blood; in these experiments a metal cannula was inserted through a trephined hole in the skull into the confluence of the sinuses and held in place by a threaded metal holder screwed into the skull.

Following surgery the animals were immobilized by means of loose-fitting, partially bisected plaster casts and then allowed to recover from the anesthesia for at least 2 h before the initiation of the experimental procedure. Animals studied in the conscious state were kept alert by tactile stimulation as required. In the studies on anesthetized animals, anesthesia was induced again and maintained throughout the experimental procedure at the level of extinction of the corneal reflex by intravenous administration of sodium thiopental as required.

**Miscellaneous physiological and biochemical measurements.** Mean arterial blood pressure was measured by means of an air-damped mercury manometer attached to the femoral arterial catheter. Rectal temperature was monitored with a YSI Model No. 73 Tele-Thermometer (Yellow Springs Instrument Co., Yellow Springs, OH). Arterial blood hemoglobin concentration was measured by the method of EVELYN & MALLOY (1938), and hematocrit was determined from blood samples centrifuged in a Beckman Microfuge B (Beckman Instruments, Fullerton, CA). Arterial blood pH,  $p\text{CO}_2$ , and  $p\text{O}_2$  were measured in an ILS Model No. 213 pH Blood Gas Analyzer (Instrumentation Laboratory, Inc., Lexington, MA).

These physiological variables are not essential to the determination of local cerebral glucose utilization. They were measured only to evaluate the normalcy of the animal's physiological state. The normal means and standard deviations for these variables in our laboratory are as

follows: mean arterial blood pressure,  $124 \pm 7$  mm Hg.; hematocrit,  $52 \pm 3\%$ ; rectal temperature,  $36.6 \pm 0.8^\circ\text{C}$ ; arterial pH,  $7.47 \pm 0.03$ ; arterial  $p\text{CO}_2$ ,  $38 \pm 2$  Torr; and arterial  $p\text{O}_2$ ,  $84 \pm 5$  Torr. Animals with any of these variables differing from the normal mean by more than two standard deviations were excluded from the studies.

Blood glucose concentration was measured enzymatically in barium–zinc filtrates (NELSON, 1944) by means of the glucose oxidase method (SAIFER & GERSTENFELD, 1958) or the coupled glucose-dependent hexokinase–glucose-6-phosphate dehydrogenase-catalyzed reduction of  $\text{NADP}^+$  (SLEIN, 1963). Plasma glucose concentration was measured directly in plasma samples either by the same enzymatic methods or by means of a Beckman Glucose Analyzer (Beckman Instruments, Fullerton, CA). Plasma and blood [ $^{14}$ C]DG concentrations were determined by assay of the  $^{14}\text{C}$  contents in measured volumes of plasma and barium–zinc filtrates of whole blood, respectively, in a liquid scintillation counter. The phosphor solution consisted of 125 g of naphthalene, 12 g of 2,5-diphenyloxazole, and 0.3 g of *p*-bis-[2-(5-phenyloxazolyl)]-benzene per liter of *p*-dioxane. The number of nCi per sample was computed from its counting rate on the basis of internal standardization with a calibrated [ $^{14}$ C]toluene standard.

**Measurement of tissue  $^{14}\text{C}$  concentration.** The  $^{14}\text{C}$  concentrations in localized regions of the brain were measured by a modification of the quantitative autoradiographic technique previously described (REIVICH *et al.*, 1969). At the selected time for the measurement the animal was decapitated, and the brain was dissected out as rapidly as possible and frozen in Freon XII chilled to  $-75^\circ\text{C}$ . When completely frozen, the brain was coated with chilled embedding medium (Lipshaw Manufacturing Co., Detroit, MI) and fixed to object-holders appropriate to the microtome to be used. The brains were then placed in plastic bags and stored at  $-70^\circ\text{C}$  until sectioned.

Brain sections, precisely  $20\ \mu\text{m}$  in thickness, were prepared in an American Optical Co. (Buffalo, NY) cryostat maintained at  $-21$  to  $-22^\circ\text{C}$ . The brain sections were picked up on glass cover slips, dried on a hot plate at  $60^\circ\text{C}$  for at least 5 min, and placed sequentially in an X-ray cassette. A set of [ $^{14}\text{C}$ ]methyl methacrylate standards (Amersham/Searle Corp., Arlington Heights, IL), which included a blank and a series of progressively increasing  $^{14}\text{C}$  concentrations, was also placed in the cassette. These standards had previously been calibrated for their autoradiographic equivalence to the  $^{14}\text{C}$  concentrations in brain sections,  $20\ \mu\text{m}$  in thickness, prepared as described above. The method of calibration has been previously described (REIVICH *et al.*, 1969).

Autoradiographs were prepared from these sections directly in the X-ray cassette with Kodak single coated, blue-sensitive Medical X-Ray Film, Type SB-54 (Eastman Kodak Co., Rochester, NY). The exposure time was generally 5–6 days, and the exposed film was developed according to the instructions supplied with the film. The autoradiographs provided a pictorial representation of the relative  $^{14}\text{C}$  concentrations in the various cerebral structures and the plastic standards (Fig. 2). A calibration curve of the relationship between optical density and tissue  $^{14}\text{C}$  concentration for each film was obtained by densitometric measurements of the portions of the film representing the various standards. The local tissue concentrations were then determined from the calibration curve and the optical densities of the film in the regions representing the cerebral structures of interest. The densitometric measurements





FIG. 2. Autoradiograph of sections of conscious rat brain and of calibrated [ $^{14}\text{C}$ ]methyl methacrylate standards used to quantify  $^{14}\text{C}$  concentration in tissues.



FIG. 6

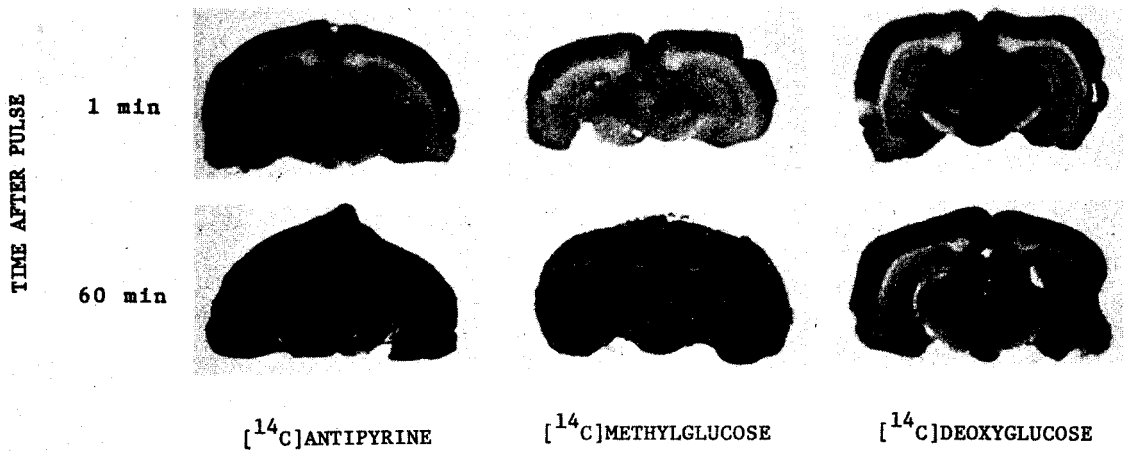


FIG. 7

were made with a Photovolt Model No. 520-A Densitometer (Photovolt Corp., New York, NY) equipped with a 0.2 mm aperture.

**Determination of  $k_1^*$ ,  $k_2^*$ , and  $k_3^*$ .** The method used to determine  $k_1^*$ ,  $k_2^*$ , and  $k_3^*$  for the various cerebral tissues was based on Equation (11), which describes the time course of the total  $^{14}\text{C}$  concentration in the tissue as a function of time, the history of the arterial plasma  $^{14}\text{C}$ ]DG concentration, and the three rate constants. If the time courses of the tissue and plasma concentrations are known, then the three rate constants can be estimated by non-linear, least squares fitting routines. Because only a single measurement of the  $^{14}\text{C}$  concentration in the cerebral tissues was possible in any one animal, the studies were carried out in a group of 15 rats matched for age and weight. Each animal was infused intravenously at a constant rate with a total dose of 20–50  $\mu\text{Ci}$  of  $^{14}\text{C}$ ]DG for 5, 10, 20, 30, or 45 min and decapitated at the end of that time. There were three animals studied for each period. Timed arterial blood samples were drawn during the infusion and assayed for plasma  $^{14}\text{C}$  content to determine the time course of the plasma  $^{14}\text{C}$ ]DG concentration prior to the time of killing. The local cerebral  $^{14}\text{C}$  concentrations at the time of decapitation were determined by the quantitative autoradiographic technique. The cerebral tissue  $^{14}\text{C}$  concentrations and the time courses of the plasma  $^{14}\text{C}$ ]DG concentration obtained from all the rats were then fitted to Equation (11). The values for  $k_1^*$ ,  $k_2^*$ , and  $k_3^*$  that provided the least squares best-fit of the equation to the experimental data were obtained in a PDP-10 computer by means of a non-linear iterative process employing the MLAB program (KNOTT & SHRAGER, 1972; KNOTT & REECE, 1972).

**Determination of the lumped constant.** The design of the procedures used to determine the lumped constant,  $\lambda V_m^* K_m / \phi V_m K_m^*$ , was based on Equations (38) and (40). These equations state that if the  $^{14}\text{C}$ ]DG is administered in such a way that its concentration in arterial plasma achieves and maintains a constant level for a sufficiently long time, the concentrations of free  $^{14}\text{C}$ ]DG and its rates of phosphorylation in the tissues will reach a steady state like that already existing for glucose. When steady states exist for both  $^{14}\text{C}$ ]DG and glucose, then the ratio of the cerebral extraction ratio of  $^{14}\text{C}$ ]DG to that of glucose, corrected by the ratio of the specific activities (i.e. ratio of  $^{14}\text{C}$ ]DG to glucose concentrations) in arterial blood and plasma, becomes equal to the lumped constant (Equation [40]). In other words, the lumped constant is really the constant of proportionality between the steady state

rates of  $^{14}\text{C}$ ]DG and glucose phosphorylation by the brain when it is exposed to equal arterial plasma concentrations of both.

In order to determine the lumped constant, it was first necessary to design an intravenous infusion schedule that would produce and maintain a constant concentration of  $^{14}\text{C}$ ]DG in the arterial plasma. Rats were, therefore, administered intravenous pulses of  $^{14}\text{C}$ ]DG, and timed arterial blood samples were drawn for at least 45 min for the measurement of the plasma  $^{14}\text{C}$ ]DG concentrations. The plasma disappearance curve was then fitted by an iterative, non-linear least squares routine to the sum of three or four exponential terms. From a Laplace transform of the relationship between the impulse input and the multi-exponential output, it was possible to compute the input function, e.g. the infusion schedule, necessary to achieve a constant arterial plasma level. The details of the mathematical procedures have been published separately (PATLAK & PETTIGREW, 1976). The infusion schedule prescribed an intravenous pulse of  $^{14}\text{C}$ ]DG followed by a continuous infusion with specified changes in rate every minute. The controlled infusion was achieved by means of a calibrated peristaltic pump with a speed control that was changed manually every minute.

Lumped constants were determined in 15 conscious and 9 anesthetized rats. Constant arterial concentrations were achieved by the appropriate intravenous infusion schedules as illustrated in Fig. 3. The initial pulse was 3–6  $\mu\text{Ci}$  of  $^{14}\text{C}$ ]DG followed by the prescribed infusion for 45 min. During the infusion times arterial and cerebral venous blood samples were drawn from the femoral artery and confluence of the sinuses, respectively. Part of each blood sample was centrifuged immediately in the Beckman Microfuge to separate the plasma, and the blood and plasma samples were assayed for their  $^{14}\text{C}$ ]DG and glucose concentrations as described above. The data were plotted as illustrated in Fig. 4, and the lumped constant was determined from the mean of the individual values of  $(E^*/E)(C_A^*/C_A)/(C_P^*/C_P)$  after it had appeared to reach its asymptotic value (Fig. 4B).

**Measurement of local cerebral glucose utilization.** Equation (30) is the operational equation of the method. It specifies the variables to be measured in order to determine  $R_i$ , the local rate of glucose consumption in the brain. The following variables are measured in each experiment: (1) the entire history of the arterial plasma  $^{14}\text{C}$ ]deoxyglucose concentration,  $C_P^*$ , from zero time to the time of killing,  $\tau$ ; (2) the steady state arterial plasma glucose level,  $C_P$ , over the same interval; and (3) the local concentration

#### Legends for Figures on p. 906

FIG. 6. Autoradiographic visualization of the effects of thiopental-anesthesia on local cerebral glucose utilization in the rat brain. The autoradiographs are, in effect, pictorial representations of the relative rates of glucose utilization in the various regions of the brain. Upper, Section from conscious rat brain. Note marked heterogeneity, especially in gray matter, including dark, thread-like line through auditory cortex, representing neuropil. Lower, Corresponding brain section from rat under thiopental-anesthesia. Note decreased heterogeneity in gray matter and virtual disappearance of visualization of neuropil.

FIG. 7. Autoradiographs of brain sections from rats 1 and 60 min after a pulse of 51–95  $\mu\text{Ci}$  of  $^{14}\text{C}$ ]antipyrine,  $^{14}\text{C}$ ]methylglucose, or  $^{14}\text{C}$ ]deoxyglucose. Note that 60 min after the pulse only the autoradiograph from the rat receiving  $^{14}\text{C}$ ]deoxyglucose retains regional heterogeneity, indicating that local metabolism rather than blood flow and transport determines the local tissue concentrations of  $^{14}\text{C}$  at long times after a pulse of  $^{14}\text{C}$ ]deoxyglucose.

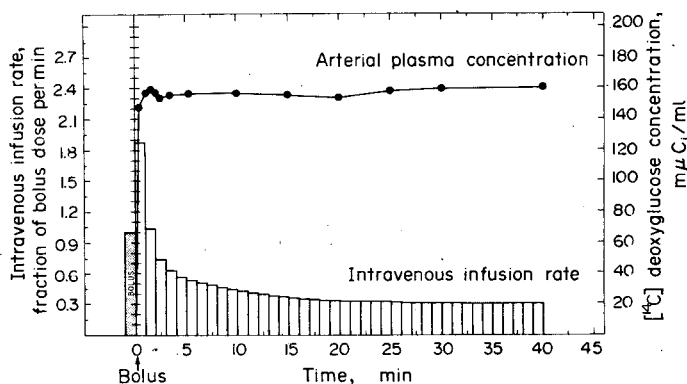


FIG. 3. Illustration of infusion schedule used to obtain constant arterial plasma concentration of [ $^{14}\text{C}$ ]deoxyglucose. The bolus contained  $3\ \mu\text{Ci}$  of [ $^{14}\text{C}$ ]deoxyglucose in  $0.3\ \text{ml}$  of physiological saline and was administered as a pulse at zero time. The infusion was continued as illustrated in the bar graph with doses equivalent to the fraction of the bolus dose indicated by the height of the bars administered at constant rates over 1-min intervals. The curve for plasma concentration represents the result obtained in a conscious rat infused according to this schedule.

of  $^{14}\text{C}$  in the tissue at the time of killing,  $C_t^*(t)$ . The rate constants,  $k_1^*$ ,  $k_2^*$ , and  $k_3^*$ , and the lumped constant,  $\lambda V_m^* K_m / \phi V_m K_m^*$ , are not measured in each experiment; the values for these constants that are used are those determined separately in other groups of animals as described above. Their values are presented in Table 1 and 2 and discussed in the Results.

Equation (30) is generally applicable with all types of arterial plasma [ $^{14}\text{C}$ ]DG concentration curves. Its configuration, however, suggests that a declining curve approaching zero by the time of killing is the choice to minimize certain potential errors. The quantitative autoradiographic technique measures only total  $^{14}\text{C}$  concentration in the tissue and does not distinguish between [ $^{14}\text{C}$ ]DG-6-P and [ $^{14}\text{C}$ ]DG. It is, however, [ $^{14}\text{C}$ ]DG-6-P concentration that must be known to determine glucose consumption. DG-6-P concentration is calculated in the numerator of Equation (30), which equals the total tissue  $^{14}\text{C}$  content,  $C_t^*(t)$ , minus the [ $^{14}\text{C}$ ]DG concentration present in the tissue, estimated by the term containing the exponential factors and rate constants. In the denominator

of Equation (30) there is also a term containing exponential factors and rate constants. Both these terms have the useful property of approaching zero with increasing time if  $C_p^*$  is also allowed to approach zero. The rate constants,  $k_1^*$ ,  $k_2^*$ , and  $k_3^*$ , have thus far been determined only in normal rats and are not measured in the same animals in which local glucose consumption is being measured. It is conceivable that these standard rate constants are not equally applicable to all rats in all physiological, pharmacological, and pathological states. One possible solution is to determine the rate constants for each condition to be studied. An alternative solution, and the one chosen, is to administer the [ $^{14}\text{C}$ ]DG as a single intravenous pulse at zero time and to allow sufficient time for the clearance of [ $^{14}\text{C}$ ]DG from the plasma and the terms containing the rate constants to fall to levels too low to influence the final result. To wait until these terms reach zero is impractical because of the long time required and the risk of effects of the small but finite rate of loss of [ $^{14}\text{C}$ ]DG-6-P from the tissues. A reasonable time interval is 45 min; by this time the plasma level has fallen to very low levels,

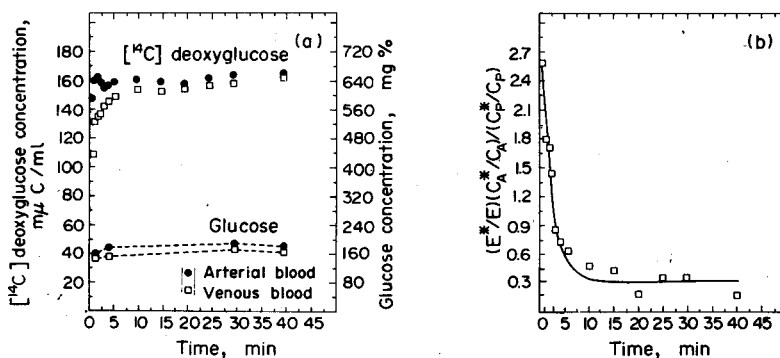


FIG. 4. Determination of lumped constant. The infusion schedule was the same as the one illustrated in Fig. 3. (A), Concentrations of [ $^{14}\text{C}$ ]deoxyglucose and glucose in arterial and cerebral venous blood. (B), Calculation of lumped constant from data in (A). The lumped constant is equal to the asymptotic value of the best-fitting curve to the individual points. See text.

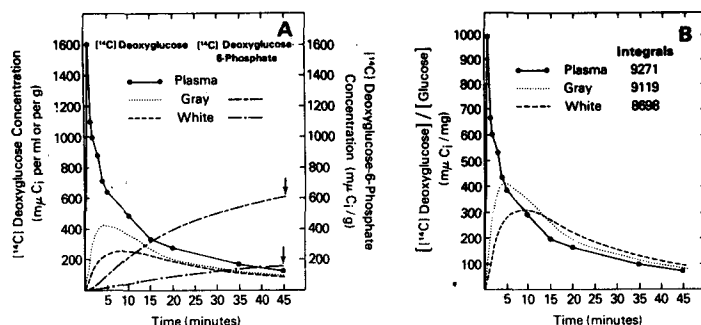


FIG. 5. Graphical representation of the significant variables in Equation (30) used to calculate local cerebral glucose utilization. (A), Time courses of  $[^{14}\text{C}]$ deoxyglucose concentrations in arterial plasma and in average gray and white matter and  $[^{14}\text{C}]$ deoxyglucose-6-phosphate concentrations in average gray and white matter following an intravenous pulse of  $50 \mu\text{Ci}$  of  $[^{14}\text{C}]$ deoxyglucose. The plasma curve is derived from measurements of plasma  $[^{14}\text{C}]$ deoxyglucose concentration. The tissue concentrations were calculated from the plasma curve and the mean values of  $k_1^*$ ,  $k_2^*$ , and  $k_3^*$  for gray and white matter in Table 1 according to Equation (8), which is equivalent to the second term in the numerator of Equation (30). The  $[^{14}\text{C}]$ deoxyglucose-6-phosphate concentrations in the tissues were calculated from the same variables and constants according to Equation (10). The arrows point to the concentrations of  $[^{14}\text{C}]$ deoxyglucose and  $[^{14}\text{C}]$ deoxyglucose-6-phosphate in the tissues at the time of killing; the autoradiographic technique measures the total  $^{14}\text{C}$  content (i.e. the sum of these concentrations) at that time, which is equal to  $C_i^*(t)$ , the first term in the numerator of Equation (30). Note that at the time of killing, the total  $^{14}\text{C}$  content represents mainly  $[^{14}\text{C}]$ deoxyglucose-6-phosphate concentration, especially in gray matter. (B), Time courses of ratios of  $[^{14}\text{C}]$ deoxyglucose to glucose concentrations (i.e. specific activities) in plasma and average gray and white matter. The curve for plasma was determined by division of the plasma curve in (A) by the plasma glucose concentrations. The curves for the tissues were calculated by the function in brackets in the denominator of Equation (29). The integrals in (B) are the integrals of the specific activities with respect to time and represent the areas under the curves. The integrals under the tissue curves are equivalent to all of the denominator of Equation (30), except for the lumped constant. Note that by the time of killing, the integrals of the tissue curves approach equality with each other and with that of the plasma curve.

and, on the basis of the values of  $(k_2^* + k_3^*)$  in Table 1, the exponential factors have declined through at least ten half-times.

The time courses of the concentrations of  $[^{14}\text{C}]$ DG and  $[^{14}\text{C}]$ DG-6-P in arterial plasma and/or representative gray and white matter following an intravenous pulse of  $[^{14}\text{C}]$ DG are illustrated in Fig. 5. As the plasma concentration falls from its peak following the pulse, the tissue concentrations of  $[^{14}\text{C}]$ DG first rise until the tissues and plasma reach equilibrium. As the plasma concentration continues to fall below its equilibrium levels, there is a net loss of  $[^{14}\text{C}]$ DG from the tissues back to the plasma, as well as continued conversion of tissue  $[^{14}\text{C}]$ DG to  $[^{14}\text{C}]$ DG-6-P, and the concentrations of free  $[^{14}\text{C}]$ DG in the tissues then decline (Fig. 5). The higher the blood flow of the tissue, the more rapidly it initially takes up  $[^{14}\text{C}]$ DG, but it reaches equilibrium with plasma sooner and loses  $[^{14}\text{C}]$ DG more rapidly after the point of equilibrium. These opposing effects of blood flow before and after equilibrium tend to cancel out the effects of blood flow. By 45 min the tissue and plasma levels of free  $[^{14}\text{C}]$ DG have reached very low levels. On the other hand, the  $[^{14}\text{C}]$ DG-6-P concentrations in the tissues rise continuously and by 45 min are responsible for most of the  $^{14}\text{C}$  in the tissues, particularly in gray matter (Fig. 5A). The numerator of Equation (30) represents the final total tissue  $^{14}\text{C}$  concentration, measured autoradiographically, minus the final point on the tissue  $[^{14}\text{C}]$ DG curve and

is equal, therefore, to the final  $[^{14}\text{C}]$ DG-6-P concentration in the tissue (Fig. 5A).

The physical significance of the denominator of Equation (30) is illustrated in Fig. 5B. The curves in Fig. 5B are derived from the curves for  $[^{14}\text{C}]$ DG concentration in plasma and average gray and white matter in Fig. 5A by dividing them by the glucose concentrations in those tissues. They represent, in effect, the time courses of the specific activities in those tissues. The integrals in Fig. 5B are the integrated specific activities, i.e. the areas under each of the curves between 0 and 45 min. The denominator of Equation (30) is equal to the product of the lumped constant and the integral appropriate to the tissue. It should be noted that the integrals for gray and white matter are almost equal to the integral for plasma (Fig. 5B). As can be seen from Equation (30), this phenomenon merely reflects the diminished contributions of the terms containing the exponential factors at 45 min after the pulse of  $[^{14}\text{C}]$ DG; at infinite time all the integrals would be equal to the integral of the plasma curve. It may be recalled that the model assumed only a single compartment for free  $[^{14}\text{C}]$ DG in each tissue. It can be shown that at infinite time following a pulse the integrals of the specific activities of all compartments, either in series or parallel, that derive their  $[^{14}\text{C}]$ DG ultimately from the plasma compartment become equal to each other and to the integral of the plasma specific activity (C. Patlak, unpublished). It would then be immaterial if there were, in-

deed, more than one compartment, and 45 min is sufficiently close to infinity (i.e. at least 10 half-times) to minimize possible errors due to that assumption.

The design of the experimental procedure for the measurement of local cerebral glucose utilization was based on all these considerations. At zero time a pulse of approx  $50^1 \mu\text{Ci}$  of  $[^{14}\text{C}]$ deoxyglucose was administered to the animal via the venous catheter. Arterial sampling was initiated with the onset of the pulse, and timed 50–100  $\mu\text{l}$  samples of arterial blood were collected consecutively as rapidly as possible during the early period so as not to miss the peak of the arterial curve. Arterial sampling was continued at more infrequent intervals later in the experimental period but at sufficient frequency to define the arterial curve. The arterial blood samples were immediately centrifuged in the Beckman Microfuge to separate the plasma, which was stored on ice until assayed for  $[^{14}\text{C}]\text{DG}$  and glucose concentrations as described above. At 45 min the animal was decapitated, the brain was removed and frozen in Freon XII chilled to  $-75^\circ\text{C}$  with liquid nitrogen. When fully frozen, the brain was stored at  $-70^\circ\text{C}$  until sectioned. The local tissue  $^{14}\text{C}$  concentrations were measured by the quantitative autoradiographic technique described above.

In some experiments the experimental period was limited to 30 min. This is theoretically permissible and may

sometimes be necessary for reasons of experimental expediency, but greater errors due to possible inaccuracies in the rate constants may result.

The final values for local cerebral glucose utilization were calculated according to Equation (30) by means of a Hewlett-Packard Model 9830A programmable calculator (Hewlett-Packard Co., Loveland, CO).

## RESULTS

### Values for $k_1^*$ , $k_2^*$ , and $k_3^*$

The least squares, best-fit estimates of  $k_1^*$ ,  $k_2^*$ , and  $k_3^*$ , for a variety of gray and white structures in the brain of the conscious rat are presented in Table 1. The values for each of the rate constants are higher in gray matter than in white matter, but within each class of structures there is relatively little variation. Therefore, to simplify computational routines only the mean values of the rate constants in gray structures and in white structures were used in the calculation of local cerebral glucose utilization in the various structures of the brain (Table 1).

The constants,  $k_2^*$  and  $k_3^*$ , always appear as their sum in Equation (30), the operational equation for the determination of local cerebral glucose utilization, and in Equation (38), the basis for the procedure for the determination of the lumped constant. ( $k_2^* + k_3^*$ ) is the exponential constant of all the exponential factors that appear in these equations. From the model and Equation (3) it can also be seen that ( $k_2^* + k_3^*$ ) is equal to the fractional turnover rate of the  $[^{14}\text{C}]\text{-DG}$  precursor pool in the tissue and can be used to calculate the half-lives of these pools. The half-lives are uniformly and significantly higher in white matter than in gray matter (Table 1). The average half-life of the precursor pool in white matter is approx 4.5 min. It was on this basis that an interval of at least 30, preferably 45 min (i.e. approx 6–10 half-lives) following the intravenous pulse of  $[^{14}\text{C}]\text{DG}$  was chosen to minimize both the contribution of free  $[^{14}\text{C}]\text{DG}$  to the autoradiographic estimates of total tissue  $^{14}\text{C}$  content and the influence of terms containing the exponential factors and rate constants on the computations of local cerebral glucose utilization by Equation (30).

The values of the rate constants have thus far been determined only in normal conscious rats. They probably vary with the condition and species of the animal. For example,  $k_3^*$  is the rate constant for the phosphorylation of  $[^{14}\text{C}]\text{DG}$  by hexokinase and must be altered by changes in metabolic rate. The values for the rate constants for the transport of  $[^{14}\text{C}]\text{DG}$  between blood and tissue,  $k_1^*$  and  $k_2^*$ , are influenced not only by the properties of the transport system but also by the steady state levels of glucose in the plasma and tissue and, to a smaller extent, by the blood flow to the tissue. For greatest accuracy, therefore, it is advisable to determine the rate constants for the condition and species of the animal desired to be studied. For studies in the rat, however, and

<sup>1</sup> The administration of  $50 \mu\text{Ci}$  of  $[^{14}\text{C}]\text{deoxyglucose}$  at a specific activity of approx  $50 \mu\text{Ci}$  per  $\mu\text{mol}$  represents a total dose of deoxyglucose of approx  $1 \mu\text{mol}$ . This is probably the maximal permissible dose for adult rats. With this dose the concentration of free deoxyglucose in gray matter may in some animals transiently rise as high as  $8 \mu\text{M}$  (Fig. 5A) and come close to violating the requirement that tracer theory apply. According to Equations (21) and (22), the theory of the method requires that the molecular concentration of free  $[^{14}\text{C}]\text{deoxyglucose}$  in the tissue be negligible compared to its  $K_m$  for hexokinase. SOLS & CRANE (1954) have reported the  $K_m$  of brain hexokinase for 2-deoxyglucose to be  $2.7 \times 10^{-5}\text{M}$ , but this value was determined with calf brain hexokinase. The  $K_m$  for rat brain hexokinase appears to be substantially higher. GROSSBARD & SCHIMKE (1966) reported the  $K_m$  value of rat brain hexokinase for 2-deoxyglucose to be  $1.1 \times 10^{-4}\text{M}$ . BACHELARD *et al.* (1971) found the inhibitor constant,  $K_i$ , of 2-deoxyglucose for glucose phosphorylation by cerebral hexokinase to equal  $0.25 \text{ mM}$ , and in the case of a competitive substrate, like deoxyglucose, the  $K_i$  is equivalent to the  $K_m$  (DIXON & WEBB, 1964). Although the tissue concentration may at times reach  $8 \mu\text{M}$ , it is only transient and sufficiently below the  $K_m$  values of  $0.11\text{--}0.25 \text{ mM}$  to allow the assumption of tracer theory without any serious error. It is, however, not negligible, and lower tissue concentrations of  $[^{14}\text{C}]\text{deoxyglucose}$  would be desirable. It is possible, of course, to use lower radioactive doses of  $[^{14}\text{C}]\text{deoxyglucose}$  or to administer the same radioactive dose of  $[^{14}\text{C}]\text{deoxyglucose}$  of higher specific activity. In the former case the  $^{14}\text{C}$  concentration in some of the tissues would have fallen below the range of the lowest calibrated autoradiographic  $[^{14}\text{C}]\text{methacrylate}$  standards available to us.  $[^{14}\text{C}]\text{Deoxyglucose}$  of higher specific activity was similarly unavailable. We are currently negotiating for commercial production of both standards with lower values and  $[^{14}\text{C}]\text{deoxyglucose}$  with higher specific activity.

TABLE 1. VALUES OF RATE CONSTANTS IN THE NORMAL CONSCIOUS ALBINO RAT†

Structure	$k_1^*$	Rate constants ( $\text{min}^{-1}$ ) $k_2^*$	$k_3^*$	Distribution vol§ (ml/g) $k_1^*/(k_2^* + k_3^*)$	Half-life of precursor pool (min) $\text{Log}_e 2/(k_2^* + k_3^*)$
Gray matter					
Visual cortex	$0.189 \pm 0.048$	$0.279 \pm 0.176$	$0.063 \pm 0.040$	0.553	2.03
Auditory cortex	$0.226 \pm 0.068$	$0.241 \pm 0.198$	$0.067 \pm 0.057$	0.734	2.25
Parietal cortex	$0.194 \pm 0.051$	$0.257 \pm 0.175$	$0.062 \pm 0.045$	0.608	2.17
Sensory-motor cortex	$0.193 \pm 0.037$	$0.208 \pm 0.112$	$0.049 \pm 0.035$	0.751	2.70
Thalamus	$0.188 \pm 0.045$	$0.218 \pm 0.144$	$0.053 \pm 0.043$	0.694	2.56
Medial geniculate body	$0.219 \pm 0.055$	$0.259 \pm 0.164$	$0.055 \pm 0.040$	0.697	2.21
Lateral geniculate body	$0.172 \pm 0.038$	$0.220 \pm 0.134$	$0.055 \pm 0.040$	0.625	2.52
Hypothalamus	$0.158 \pm 0.032$	$0.226 \pm 0.119$	$0.043 \pm 0.032$	0.587	2.58
Hippocampus	$0.169 \pm 0.043$	$0.260 \pm 0.166$	$0.056 \pm 0.040$	0.535	2.19
Amygdala	$0.149 \pm 0.028$	$0.235 \pm 0.109$	$0.032 \pm 0.026$	0.558	2.60
Caudate-putamen	$0.176 \pm 0.041$	$0.200 \pm 0.140$	$0.061 \pm 0.050$	0.674	2.66
Superior colliculus	$0.198 \pm 0.054$	$0.240 \pm 0.166$	$0.046 \pm 0.042$	0.692	2.42
Pontine gray matter	$0.170 \pm 0.040$	$0.246 \pm 0.142$	$0.037 \pm 0.033$	0.601	2.45
Cerebellar cortex	$0.225 \pm 0.066$	$0.392 \pm 0.229$	$0.059 \pm 0.031$	0.499	1.54
Cerebellar nucleus	$0.207 \pm 0.042$	$0.194 \pm 0.111$	$0.038 \pm 0.035$	0.892	2.99
Mean $\pm$ S.E.M.	$0.189 \pm 0.012$	$0.245 \pm 0.040$	$0.052 \pm 0.010$	$0.647 \pm 0.073$	$2.39 \pm 0.40$
White matter					
Corpus callosum	$0.085 \pm 0.015$	$0.135 \pm 0.075$	$0.019 \pm 0.033$	0.552	4.50
Genu of corpus callosum	$0.076 \pm 0.013$	$0.131 \pm 0.075$	$0.019 \pm 0.034$	0.507	4.62
Internal capsule	$0.077 \pm 0.015$	$0.134 \pm 0.085$	$0.023 \pm 0.039$	0.490	4.41
Mean $\pm$ S.E.M.	$0.079 \pm 0.008$	$0.133 \pm 0.046$	$0.020 \pm 0.020$	$0.516 \pm 0.171$	$4.51 \pm 0.90$

† The individual values for  $k_1^*$ ,  $k_2^*$ , and  $k_3^*$  are the estimates  $\pm$  standard errors of the estimates determined by a non-linear least squares fit of Equation (11) to the data from 15 animals (KNOTT & SHRAGER, 1972; KNOTT & REECE, 1972). The distribution volumes and the half-lives of the precursor pools were calculated from the individual rate constants as indicated. The standard errors of the means of the values for gray matter and white matter were calculated from the standard errors of the estimates of the individual rate constants and their covariances.

§ Distribution volume and distribution ratio are used interchangeably. It is the steady state ratio of tissue concentration to plasma concentration and is equal to the volume of distribution space per unit mass of tissue.

particularly in gray matter, the quantitative nature of the rate constants combined with the design of the procedure serve to permit a considerable latitude in the values of the constants around those in Table 1 without any major influence on the calculated values for local cerebral glucose utilization. Because  $k_2^*$  is so much greater than  $k_3^*$ , the pool turnover rate constant,  $k_2^* + k_3^*$ , is largely determined by  $k_2^*$  alone, and considerable fluctuation in  $k_3^*$  can occur without any major change in the half-life of the precursor pool of [ $^{14}\text{C}$ ]DG. The conditions that might alter either  $k_1^*$  or  $k_2^*$  are likely to change both in the same direction. Because of their position in the last term of the numerator of Equation (30), the effects of changes in  $k_1^*$  and  $k_2^*$  in the same direction would tend to counteract each other. Finally, by allowing a long interval following the pulse, the terms in Equation [30] that contain the rate constants become so small compared to the terms from which they are subtracted that the effects of errors in these terms are attenuated and produce relatively small percent changes in the estimated rates of glucose utilization.

The distribution ratios for [ $^{14}\text{C}$ ]DG between the plasma and the various cerebral tissues, determined from  $k_1^*/(k_2^* + k_3^*)$ , appear to be greater in gray matter than in white matter (Table 1), but in each group they are rather uniform. These distribution ratios, cal-

culated on the basis of the rate constants, agree quite well with the value, 0.575 (S.D. =  $\pm 0.019$ ), that Fishman (R. Fishman, personal communication) has found experimentally to be the average distribution ratio for the brain as a whole. This agreement provides some evidence for the reliability of the computed values for the rate constants in Table 1.

#### Evaluation of $(\lambda V_m K_m / \Phi V_m K_m^*)$

The lumped constant is determined from the ratio of the steady state fractional extractions of [ $^{14}\text{C}$ ]DG and glucose from the blood by the brain. By duplicate and triplicate determinations in each sample it was possible to measure the [ $^{14}\text{C}$ ]DG and glucose concentrations in blood and plasma with a coefficient of variation of less than 2%. Because the fractional extractions of [ $^{14}\text{C}$ ]DG and glucose by brain are small, even these low analytical errors could produce considerably greater errors in the arteriovenous differences on which the extraction ratios are based. It was, therefore, necessary to determine the lumped constant in a sufficiently large series of animals to minimize the influence of these random analytical errors. In 15 normal conscious rats, the mean and standard deviation of the lumped constant were found to be  $0.464 \pm 0.099$  (Table 2). Because it represents mainly the ratios of the Michaelis-Menten kinetic constants

of brain hexokinase for deoxyglucose and glucose (see Theory section), the lumped constant could be expected to be a constant characteristic of the species of animal. Nevertheless, the possibility that it might vary in different conditions was examined by its determination in rats under thiopental anesthesia. In a series of 9 anesthetized rats the mean  $\pm$  S.D. was  $0.512 \pm 0.118$ , not even close to statistically significant difference from the value in conscious rats (Table 2). The values for the lumped constants in the two series were, therefore, grouped together, resulting in a lumped constant for the Sprague-Dawley rat of  $0.483$  (S.E.M. =  $\pm 0.022$ ) (Table 2). This is the value used for the determination of local cerebral glucose utilization in the present studies. Preliminary results of determinations of the lumped constant in conscious Sprague-Dawley rats breathing 5% CO<sub>2</sub>, which raises cerebral blood flow and produces respiratory acidosis, indicate no change in the lumped constant under these conditions.

#### *Rates of local cerebral glucose utilization in the normal conscious rat*

One of the basic assumptions of the method is that [<sup>14</sup>C]DG-6-P is essentially trapped during the period of measurement. If this were not so, then the estimated local cerebral glucose utilization would show a time dependency and decrease with increasing duration of the experimental period. To test this assumption again, local cerebral glucose utilization was measured in normal conscious rats during 30 min and 45 min experimental periods. There were no statistically significant effects of time on the values for local cerebral glucose utilization in all but one of the 33 cerebral structures examined, further confirming the validity of the assumption (Table 3).

Local cerebral glucose utilization varied widely throughout the brain (Table 3). The values in white matter tended to group together and were always considerably below those of gray structures. The average value in gray matter was about 3 times that of white matter, but the individual values varied from approx 50 to 200  $\mu$ mol of glucose/100 g/min. The highest values were clearly in the structures involved in auditory functions with the inferior colliculus the most metabolically active structure in the brain (Table 3).

TABLE 2. EVALUATION OF LUMPED CONSTANT IN ALBINO RAT

Condition	No. of Animals	Mean $\pm$ S.D.	S.E.M.
Conscious	15	$0.464 \pm 0.099$	$\pm 0.026$
Anesthetized	9	$0.512 \pm 0.118$	$\pm 0.039$
Combined	24	$0.483 \pm 0.107$	$\pm 0.022$

No significant difference between values in conscious and anesthetized animals ( $0.4 > P > 0.3$ ).

TABLE 3. COMPARISON OF VALUES OF LOCAL CEREBRAL GLUCOSE UTILIZATION DETERMINED AT 30 AND 45 min FOLLOWING PULSE OF [<sup>14</sup>C]DEOXYGLUCOSE IN THE NORMAL CONSCIOUS RAT

Structure	30 min (10)* ( $\mu$ mol/ 100 g/min)	45 min (10)* ( $\mu$ mol/ 100 g/min)
Gray matter		
Visual cortex	$113 \pm 4$	$107 \pm 6$
Auditory cortex	$163 \pm 4$	$162 \pm 5$
Parietal cortex	$110 \pm 3$	$112 \pm 5$
Sensory-motor cortex	$124 \pm 3$	$120 \pm 5$
Olfactory cortex	$104 \pm 2$	$98 \pm 5$
Frontal cortex	$112 \pm 4$	$116 \pm 5$
Thalamus: lateral nucleus	$110 \pm 2$	$116 \pm 5$
Thalamus: ventral nucleus	$98 \pm 2$	$109 \pm 5$
Medial geniculate body	$130 \pm 4$	$131 \pm 5$
Lateral geniculate body	$94 \pm 2$	$96 \pm 5$
Hypothalamus	$61 \pm 2$	$54 \pm 2^\dagger$
Mamillary body	$123 \pm 4$	$121 \pm 5$
Hippocampus:		
ammon's horn	$79 \pm 1$	$79 \pm 3$
Hippocampus:		
dentate gyrus	$70 \pm 2$	$67 \pm 3$
Amygdala	$54 \pm 2$	$52 \pm 2$
Septal nucleus	$62 \pm 1$	$64 \pm 3$
Caudate-putamen	$111 \pm 2$	$110 \pm 4$
Nucleus accumbens	$83 \pm 3$	$82 \pm 3$
Globus-pallidus	$58 \pm 3$	$58 \pm 2$
Substantia nigra	$61 \pm 2$	$58 \pm 3$
Vestibular nucleus	$134 \pm 3$	$128 \pm 5$
Cochlear nucleus	$128 \pm 5$	$113 \pm 7$
Superior olivary nucleus	$147 \pm 6$	$133 \pm 7$
Lateral lemniscus	$114 \pm 5$	$104 \pm 5$
Inferior colliculus	$203 \pm 6$	$197 \pm 10$
Superior colliculus	$100 \pm 3$	$95 \pm 5$
Pontine gray matter	$69 \pm 2$	$62 \pm 3$
Cerebellar cortex	$63 \pm 2$	$57 \pm 2$
Cerebellar nucleus	$106 \pm 3$	$100 \pm 4$
White matter		
Corpus callosum	$39 \pm 2$	$40 \pm 2$
Genu of corpus callosum	$35 \pm 3$	$34 \pm 1$
Internal capsule	$33 \pm 2$	$33 \pm 2$
Cerebellar white matter	$37 \pm 1$	$37 \pm 2$

\* The values are the means  $\pm$  standard errors from measurements made in the number of animals indicated in brackets.

† Statistically significant difference ( $P < 0.05$ ).

#### *Effects of anesthesia on local cerebral glucose utilization*

Thiopental anesthesia reduced the rates of glucose utilization in all structures of the brain examined (Table 4). The effects were not uniform; the percent effects in white matter were relatively small compared to those in most gray structures. Anesthesia also markedly reduced the heterogeneity normally present within gray matter, an effect clearly visible in the autoradiographs (Fig. 6). These results are in agreement with those of previous studies in which anesthesia has been found to decrease the cerebral metabolic rate of the brain as a whole (KETTY, 1950; LASSEN, 1959; SOKOLOFF, 1976).



TABLE 4. EFFECTS OF THIOPENTAL ANESTHESIA ON LOCAL CEREBRAL GLUCOSE CONSUMPTION IN THE ALBINO RAT\*

Structure	Local cerebral glucose utilization ( $\mu\text{mol}/100\text{ g/min}$ )		
	Control (6)†	Anesthetized (8)†	% Effect
Gray matter			
Visual cortex	111 $\pm$ 5	64 $\pm$ 3	-42
Auditory cortex	157 $\pm$ 5	81 $\pm$ 3	-48
Parietal cortex	107 $\pm$ 3	65 $\pm$ 2	-39
Sensory-motor cortex	118 $\pm$ 3	67 $\pm$ 2	-43
Lateral geniculate body	92 $\pm$ 2	53 $\pm$ 3	-42
Medial geniculate body	126 $\pm$ 6	63 $\pm$ 3	-50
Thalamus: lateral nucleus	108 $\pm$ 3	58 $\pm$ 2	-46
Thalamus: ventral nucleus	98 $\pm$ 3	55 $\pm$ 1	-44
Hypothalamus	63 $\pm$ 3	43 $\pm$ 2	-32
Caudate-putamen	111 $\pm$ 4	72 $\pm$ 3	-35
Hippocampus: ammon's horn	79 $\pm$ 1	56 $\pm$ 1	-29
Amygdala	56 $\pm$ 4	41 $\pm$ 2	-27
Cochlear nucleus	124 $\pm$ 7	79 $\pm$ 5	-36
Lateral lemniscus	114 $\pm$ 7	75 $\pm$ 4	-34
Inferior colliculus	198 $\pm$ 7	131 $\pm$ 8	-34
Superior olivary nucleus	141 $\pm$ 5	104 $\pm$ 7	-26
Superior colliculus	99 $\pm$ 3	59 $\pm$ 3	-40
Vestibular nucleus	133 $\pm$ 4	81 $\pm$ 4	-39
Pontine gray matter	69 $\pm$ 3	46 $\pm$ 3	-33
Cerebellar cortex	66 $\pm$ 2	44 $\pm$ 2	-33
Cerebellar nucleus	106 $\pm$ 4	75 $\pm$ 4	-29
White matter			
Corpus callosum	42 $\pm$ 2	30 $\pm$ 2	-29
Genu of corpus callosum	35 $\pm$ 5	30 $\pm$ 2	-14
Internal capsule	35 $\pm$ 2	29 $\pm$ 2	-17
Cerebellar white matter	38 $\pm$ 2	29 $\pm$ 2	-24

\* Determined at 30 min following pulse of [ $^{14}\text{C}$ ]deoxyglucose.

† The values are the means  $\pm$  standard errors obtained in the number of animals indicated in brackets. All the differences are statistically significant at the  $P < 0.05$  level.

## DISCUSSION

The present method provides the means to measure simultaneously the rates of glucose consumption in all the macroscopic structures of the brain of laboratory animals, even in the conscious state. An unusual feature of the method is its use of a labeled analogue to trace not the route but the rate of metabolism of a natural substrate through its metabolic pathway. This is, in fact, the basic principle of the method. The analogue is one with special properties. It is metabolized in competition with the natural substrate through one or more steps of the metabolic pathway until it is eventually converted to a labeled product that cannot be further metabolized and accumulates in the tissue. The metabolism of the natural substrate must be in a steady state, and the labeled analogue and its products must be present in tracer amounts. The amount of accumulated product represents the integrated rate of metabolism of the analogue through the enzymatic step that produces it. This integral bears a quantitative relationship to the steady state flux of the natural metabolic pathway through that step that depends on the relative concentrations of the analogue and normal substrate in the precursor

pool and the ratios of the enzyme's kinetic constants for the two substrates. The exact nature of the quantitative relationship is given by Equation (30). It is essentially the same relationship that would apply to the kinetics of tracers with isotope effects. In the present studies these principles have been applied to the pathway of glucose metabolism. It is likely that the same principles are more generally applicable and that comparable methods can be designed for other metabolic pathways.

The validity of any method rests ultimately on the accuracy of the results that it provides, but there are few comparable data with which to assess the accuracy of the present results. There are published data on the average rates of glucose and oxygen consumption in the brain of the rat as a whole. In studies with a modification of the Kety-Schmidt technique, EKLÖF *et al.* (1973) reported a rate of oxygen consumption of 10.2 ml/100 g/min in the whole cerebral cortex of rats lightly anesthetized with 70%  $\text{N}_2\text{O}$ -30%  $\text{O}_2$ . In similar studies NILSSON & SIESJÖ (1976) and GJEDDE *et al.* (1975) found the oxygen consumption of the brain as a whole to be 7.6 and 5.4 ml  $\text{O}_2$ /100 g/min, respectively. If the stoichiometry

between cerebral  $O_2$  consumption and glucose utilization is close to 6 mol per mol, respectively, in the rat as it is in man (KETY, 1957; SOKOLOFF, 1976), then the rates of cerebral glucose consumption in these animals would have been between 40 and 80  $\mu\text{mol}/100\text{ g}/\text{min}$ . With their  $[2\text{-}^{14}\text{C}]\text{glucose}$  technique HAWKINS *et al.* (1974) found a mean cerebral glucose utilization of 62  $\mu\text{mol}/100\text{ g}/\text{min}$  in conscious rats. These published values for the brain as a whole could be compared directly with the present results only if it were possible to calculate the mean of the individual local rates of glucose consumption weighted for the relative masses of the structures. Inasmuch as these weighting factors are unknown for the rat brain, direct comparison is impossible. It is apparent, however, that the values for local cerebral glucose utilization in the conscious rat obtained with the present method are distributed around the mean values reported in the literature for the brain as a whole.

In order to achieve a more direct evaluation of the accuracy of the  $[^{14}\text{C}]\text{DG}$  technique Collins (R. C. Collins, personal communication) has measured the rate of glucose consumption only in the visual cortex of conscious albino rats by means of adaptations of the LOWRY closed system technique (1964) and the  $[2\text{-}^{14}\text{C}]\text{glucose}$  method of HAWKINS *et al.* (1974). He obtained values of 115  $\mu\text{mol}/100\text{ g}/\text{min}$  with the Lowry technique and 80  $\mu\text{mol}/100\text{ g}/\text{min}$  with the  $[2\text{-}^{14}\text{C}]\text{glucose}$  method. These two methods probably establish the limits of the range within which the rate of glucose consumption must lie. The Lowry technique may over-estimate the value because of a stimulation of glycolysis by tissue hypoxia during the interval between decapitation and freezing of the brain. The  $[2\text{-}^{14}\text{C}]\text{glucose}$  technique errs in the low direction because of the invalidity of two of its assumptions, no loss of  $^{14}\text{C}$  from the brain for at least 7 min after the entry of  $[2\text{-}^{14}\text{C}]\text{glucose}$  into the brain, and instantaneous and sustained isotopic equilibrium between the  $[^{14}\text{C}]\text{glucose}$  pools in the tissue and plasma throughout the period of the experiment. It is reassuring that 107  $\mu\text{mol}/100\text{ g}/\text{min}$ , the value for local cerebral glucose utilization in the visual cortex, obtained with the  $[^{14}\text{C}]\text{DG}$  technique (Table 3), falls between these limits.

Blood flow often critically influences the rates of exchange of substances between the blood and tissues, and the question may arise whether the results obtained with the  $[^{14}\text{C}]\text{DG}$  technique might not reflect more local blood flow than metabolic rate. Local cerebral blood flow normally does correlate closely with local cerebral glucose utilization (DES ROSIERS *et al.*, 1974), but it has little direct influence on the results obtained with the  $[^{14}\text{C}]\text{DG}$  technique. First of all, blood flow influences the rate of exchange between blood and tissue only by its effects on the concentration gradient between capillary blood and tissue. These effects are mediated by its influence on mean capillary concentration, the higher the blood flow the closer the mean capillary concentration to

that of arterial blood. For substances with normally low extraction ratios, like  $[^{14}\text{C}]\text{DG}$ , the mean capillary concentration is already so close to that of arterial blood that blood flow has very little influence on it, except in conditions of disproportionately reduced blood flow relative to metabolic rate when the arteriovenous difference may be increased. Secondly, the design of the procedure, i.e. the use of a pulse of  $[^{14}\text{C}]\text{DG}$  followed by a long interval, serves to eliminate the influence of blood flow. Immediately following the pulse before isotopic equilibrium between plasma and tissue is reached, higher blood flow enhances the rate of uptake of the tracer and accelerates the achievement of equilibrium (Fig. 5B). Following equilibration the plasma level falls below the equilibrium level, and higher blood flow accelerates the clearance of the free  $[^{14}\text{C}]\text{DG}$  from the tissue (Fig. 5B). With sufficiently long intervals after the pulse, the opposing effects of blood flow on uptake of  $[^{14}\text{C}]\text{DG}$  by the tissues before and after equilibrium tend to cancel each other out and with them the influence of blood flow on the calculated rates of local cerebral glucose utilization. This phenomenon can be explained more precisely in mathematical terms. The influence of blood flow is manifested in the values of the rate constants,  $k_1^*$  and  $k_2^*$ . The procedure of a pulse followed by a long interval was specifically selected to reduce the terms in Equation [30] that contain these constants to negligible levels and to minimize their influence and, therefore, also that of blood flow on the values for local cerebral glucose utilization calculated by that equation. Finally, the possible influence of blood flow was examined by direct experimental means. Pulses of  $[^{14}\text{C}]\text{antipyrine}$ , 3- $O$ - $[^{14}\text{C}]\text{methylglucose}$ , or  $[^{14}\text{C}]\text{-deoxyglucose}$  were administered to conscious rats, the animals were decapitated one or 60 min later, and their brains were sectioned and autoradiographed. The  $[^{14}\text{C}]\text{antipyrine}$  was used to trace the effects of blood flow alone on the autoradiographs (REIVICH *et al.*, 1969). The  $[^{14}\text{C}]\text{methylglucose}$ , which is transported across the blood-brain barrier by the same carrier that transports glucose and  $[^{14}\text{C}]\text{DG}$  (BIDDER, 1968; BACHELARD, 1971; OLDENDORF, 1971), was used to trace the effects of blood flow and transport. The  $[^{14}\text{C}]\text{DG}$  traces the effects of blood flow, transport, and metabolism. At one minute after the pulses all the autoradiographs were almost indistinguishable; all showed the same heterogeneous distribution of  $^{14}\text{C}$ , and the effects of metabolism could not be distinguished from those of blood flow (Fig. 7). After 60 min, however, the autoradiographs obtained with  $[^{14}\text{C}]\text{antipyrine}$  and  $[^{14}\text{C}]\text{methylglucose}$  were similar and of uniform density, but the autoradiograph with  $[^{14}\text{C}]\text{deoxyglucose}$  exhibited the same heterogeneous distribution of  $^{14}\text{C}$  generally seen with the  $[^{14}\text{C}]\text{DG}$  technique (Fig. 7). Inasmuch as  $[^{14}\text{C}]\text{DG}$  differs from the other compounds only in that it is phosphorylated, it is clear from the autoradiographs that its uptake under the conditions of the  $[^{14}\text{C}]\text{DG}$

technique reflects its metabolism and not blood flow.

It should be reemphasized that the [ $^{14}\text{C}$ ]DG technique measures only the rate of utilization of glucose taken up by the cerebral tissues from the blood. In a steady state, the net rate of glucose uptake from the blood equals the rate of glucose consumption. The method is valid for energy metabolism only in such steady states. During conditions of net glycogenolysis or glycogen accumulation, for example, the technique will underestimate or overestimate, respectively, the rate of glucose utilization used for energy metabolism.

The present report describes only the application of the [ $^{14}\text{C}$ ]DG technique to the rat for which the lumped constant and the rate constants have been determined. The method can be applied to other species as well, but for full quantification these constants must first be evaluated in each species. Studies are currently in progress to determine them in the cat and monkey. Preliminary results indicate that their values will be similar, though not identical, to those of the rat. The development of computerized emission tomography raises the possibility that the method can also be applied to man, provided that a  $\gamma$ -emitting analogue of glucose with biochemical properties like that of deoxyglucose can be obtained. Experiments in rats with 2-fluoro-2-deoxy-D-[ $^{14}\text{C}$ ]glucose have demonstrated that it behaves just like [ $^{14}\text{C}$ ]deoxyglucose in the present method, except that it is associated with a lower lumped constant. Preliminary results of experiments in man with the  $\gamma$ -emitting analogue, 2-[ $^{18}\text{F}$ ]fluoro-2-deoxy-D-glucose, combined with emission tomography provide encouraging evidence that the method can be applied to man (M. Reivich, D. Kuhl, A. Wolf, J. Greenberg, M. Phelps, T. Ido, V. Casella, J. Fowler, B. Gallagher, E. Hoffman, A. Alavi & L. Sokoloff, unpublished observations).

Because of the use of a pulse followed by a long interval before decapitation of the animal, the autoradiographs reflect primarily the concentrations of [ $^{14}\text{C}$ ]deoxyglucose-6-phosphate in the various structures of the brain. The autoradiographs are, therefore, pictorial representations of the relative rates of glucose consumption throughout the brain. Experiments with the technique have demonstrated that experimentally induced alterations in local functional activity in the CNS are associated with corresponding changes in local rates of glucose consumption that can be visualized directly on the autoradiographs without the need for quantification. By the use of positive and negative evoked metabolic responses it has been possible to map functionally related elements of the CNS and to identify regions of altered functional and metabolic activities in various physiological and pathological states (KENNEDY *et al.*, 1975; PLUM *et al.*, 1976; COLLINS *et al.*, 1976). The [ $^{14}\text{C}$ ]deoxyglucose method has proved effective in mapping the visual system of the monkey and has dramatically demonstrated the nature and distribution of the ocular dominance columns (KENNEDY *et*

*al.*, 1976). Thus far the resolution has been only at the macroscopic level. With refinements of the autoradiographic procedures it may prove possible to attain a microscopic level of resolution.

**Acknowledgements**—The authors are indebted to JANE W. JEHL and GWEN CARBIN for their skillful technical assistance in the preparation of the brain sections and autoradiographs, to SUZANNE M. COOK for her great skill and patience in the preparation of the typescript, particularly the formidable mathematical expressions, and to RUTH BOWER for her valuable bibliographic assistance.

## REFERENCES

- BACHELARD H. S. (1971) *J. Neurochem.* **18**, 213–222.
- BACHELARD H. S., CLARK A. G. & THOMPSON M. F. (1971) *Biochem. J.* **123**, 707–715.
- BIDDER T. G. (1968) *J. Neurochem.* **15**, 867–874.
- COLLINS R. C., KENNEDY C., SOKOLOFF L. & PLUM F. (1976) *Archs Neurol.* **33**, 536–542.
- DES ROSIERS M. H., KENNEDY C., PATLAK C. S., PETTIGREW K. D., SOKOLOFF L. & REIVICH M. (1974) *Neurology* **24**, 389.
- DIXON M. & WEBB E. C. (1964) *Enzymes*, 2nd Ed., pp. 84–87. Academic Press, New York.
- EKLÖF B., LASSEN N. A., NILSSON L., NORBERG K. & SIESJÖ B. K. (1973) *Acta physiol. scand.* **88**, 587–589.
- EVELYN K. A. & MALLOY H. T. (1938) *J. biol. Chem.* **126**, 655–662.
- FREYGANG W. H. & SOKOLOFF L. (1958) *Adv. biol. med. Phys.* **6**, 263–279.
- GJEDDE A., CARONNA J. J., HINDFELT B. & PLUM F. (1975) *Am. J. Physiol.* **229**, 113–118.
- GROSSBARD L. & SCHIMKE R. T. (1966) *J. biol. Chem.* **241**, 3546–3560.
- HAWKINS R. A., MILLER A. L., CREMER J. E. & VEECH R. L. (1974) *J. Neurochem.* **23**, 917–923.
- HERS H. G. & DE DUVE C. (1950) *Bull. Soc. chim. Biol.* **32**, 20–29.
- HERS H. G. (1957) *Le Métabolisme du Fructose*, p. 102. Editions Arscia, Bruxelles.
- HORTON R. W., MELDRUM B. S. & BACHELARD H. S. (1973) *J. Neurochem.* **21**, 507–520.
- KENNEDY C., DES ROSIERS M., PATLAK C. S., PETTIGREW K. D., REIVICH M. & SOKOLOFF L. (1974) *Trans. Am. Soc. Neurochem.* **5**, 86.
- KENNEDY C., DES ROSIERS M. H., REIVICH M., SHARP F., JEHL J. W. & SOKOLOFF L. (1975) *Science* **187**, 850–853.
- KENNEDY C., DES ROSIERS M. H., SAKURADA O., SHINOHARA M., REIVICH M., JEHL J. W. & SOKOLOFF L. (1976) *Proc. natn. Acad. Sci., U.S.A.* **73**, 4230–4234.
- KETY S. S. & SCHMIDT C. F. (1948) *J. clin. Invest.* **27**, 476–483.
- KETY S. S. (1950) *Am. J. Med.* **8**, 205–217.
- KETY S. S. (1957) in *The Metabolism of the Nervous System* (RICHTER D., ed.) pp. 221–237. Pergamon Press, London.
- KETY S. S. (1960) *Meth. Med. Res.* **8**, 228–236.
- KNOTT G. D. & REECE D. K. (1972) in *Proc. ONLINE '72 International Conference*, Vol. 1, pp. 497–526. Brunel University, England.
- KNOTT G. D. & SHRAGER R. I. (1972) in *Computer Graphics: Proc. SIGGRAPH Computers in Medicine Symposium*, Vol. 6, No. 4, pp. 138–151. ACM, SIGGRAPH Notices.

- LANDAU B. R. & LUBS H. A. (1958) *Proc. Soc. exp. Biol.*, N.Y. **99**, 124-127.
- LANDAU W. H., FREYGANG W. H., ROWLAND L. P., SOKOLOFF L. & KETY S. S. (1955) *Trans. Am. Neurol. Ass.* **80**, 125-129.
- LASSEN N. A. & MUNCK O. (1955) *Acta physiol. scand.* **33**, 30-49.
- LASSEN N. A. (1959) *Physiol. Rev.* **39**, 183-238.
- LOWRY O. H., PASSONNEAU J. V., HASSELBERGER F. X. & SCHULZ D. W. (1964) *J. biol. Chem.* **239**, 18-30.
- MELDRUM B. S. & HORTON R. W. (1973) *Electroenceph. clin. Neurophysiol.* **35**, 59-66.
- NELSON N. (1944) *J. biol. Chem.* **153**, 375-380.
- NILSSON B. & SIESJÖ B. K. (1976) *Acta physiol. scand.* **96**, 72-82.
- OLDENDORF W. H. (1971) *Am. J. Physiol.* **221**, 1629-1638.
- PATLAK C. S. & PETTIGREW K. D. (1976) *J. Appl. Physiol.* **40**, 458-463.
- PLUM F., GJEDDE A. & SAMSON F. E. (1976) *Neurosci. Res. Prog. Bull.* **14**, 457-518.
- PRASANNAN K. G. & SUBRAHMANYAM K. (1968) *Endocrinology* **82**, 1-6.
- RAGGI F., KRONFELD D. S. & KLEIBER M. (1960) *Proc. Soc. exp. Biol. Med.* **105**, 485-486.
- REIVICH M., JEHL J. W., SOKOLOFF L. & KETY S. S. (1969) *J. appl. Physiol.* **27**, 296-300.
- SAIFER A. & GERSTENFELD S. (1958) *J. Lab. Clin. Med.* **51**, 448-460.
- SCHEINBERG P. & STEAD E. A., JR. (1949) *J. clin. Invest.* **28**, 1163-1171.
- SLEIN M. W. (1963) in *Methods of Enzymatic Analysis* (BERGMEYER H. U., ed.) pp. 117-123. Academic Press, New York.
- SOKOLOFF L. (1960) in *Handbook of Physiology-Neurophysiology* (FIELD J., MAGOUN H. W. & HALL V. E., eds.) Vol. III, pp. 1843-1864. American Physiological Society, Washington DC.
- SOKOLOFF L. (1969) in *Psychochemical Research in Man* (MANDELL A. J. & MANDELL M. P., eds.) pp. 237-252. Academic Press, New York.
- SOKOLOFF L., REIVICH M., PATLAK C. S., PETTIGREW K. D., DES ROSIERS M. & KENNEDY C. (1974) *Trans. Am. Soc. Neurochem.* **5**, 85.
- SOKOLOFF L. (1976) in *Basic Neurochemistry*, (SIEGEL G. J., ALBERS R. W., KATZMAN R. & AGRANOFF B. W., eds.) 2nd Ed., pp. 388-413. Little, Brown, Boston.
- SOLS A. & CRANE R. K. (1954) *J. biol. Chem.* **210**, 581-595.
- TOWER D. B. (1958) *J. Neurochem.* **3**, 185-205.
- WICK A. N., DRURY D. R., NAKADA H. I. & WOLFE J. B. (1957) *J. biol. Chem.* **224**, 963-969.